



Multiple eco-regions contribute to the seasonal cycle of Antarctic aerosol size distributions

James Brean¹, David C. S. Beddows¹, Eija. Asmi², Aki Virkkula^{2,3}, Lauriane L. J. Quéléver³, Mikko Sipilä³, Floortje Van Den Heuvel⁴, Thomas Lachlan-Cope⁴, Anna E. Jones⁴, Markus Frey⁴, Angelo Lupi⁵, Jiyeon Park⁶, Young Jun Yoon⁶, Rolf Weller⁷, Giselle L. Marinovich^{8,9}, Gabriela C. Mulena^{8,9}, Roy M. Harrison^{1,+} and Manuel Dall'Osto^{10*}

¹School of Geography, Earth, and Environmental Sciences, University of Birmingham, Edgbaston, Birmingham, B15 2TT, United Kingdom

²Finnish Meteorological Institute, FI-00101 Helsinki, Finland

³Institute for Atmospheric and Earth System Research, University of Helsinki Helsinki, FI-00014, Finland

⁴British Antarctic Survey, NERC, High Cross, Madingley Rd, Cambridge, CB3 0ET, United Kingdom

⁵Institute of Polar Science (IPS), National Research Council (CNR), Venezia, Italy

⁶Korea Polar Research Institute, 26, SongdoMirae-ro, Yeonsu-Gu, Incheon, KOREA 406-840

⁷AWI, Germany

⁸Servicio Meteorológico Nacional (SMN), Av. Dorrego 4019, Buenos Aires, Argentina

⁹Consejo Nacional de Investigaciones Científicas y Técnicas (CONICET), Argentina

¹⁰Institute of Marine Sciences, CSIC, Barcelona, Spain

*Also at: Department of Environmental Sciences/Centre of Excellence in Environmental Studies, King Abdulaziz University, PO Box 80203, Jeddah, 21589, Saudi Arabia.

25

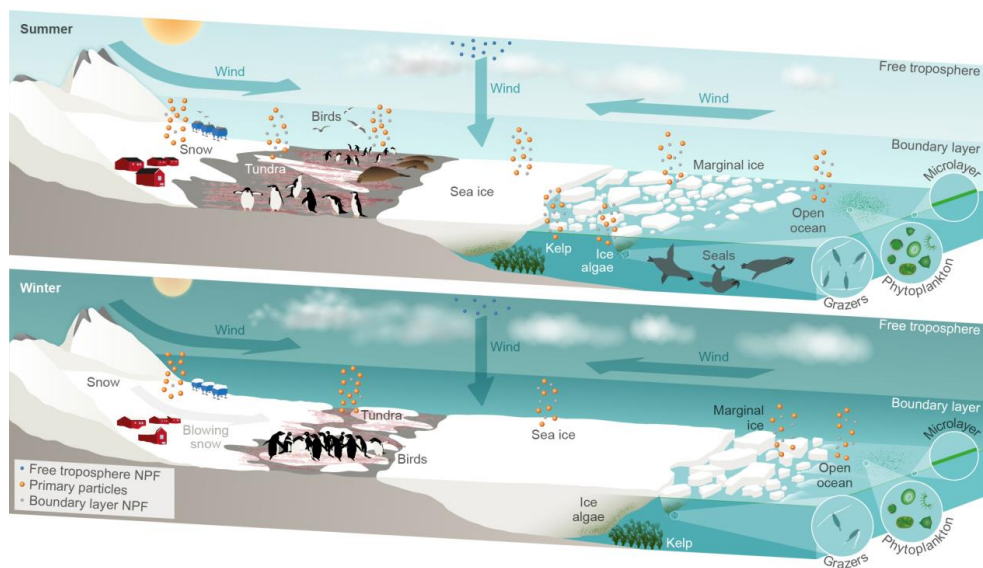
*Correspondence to dallosto@icm.csic.es



30

35

Graphical abstract



40

45



Abstract

In order to reduce the uncertainty of aerosol radiative forcing in global climate models, we need to better understand natural aerosol sources which are important to constrain the current and pre-industrial climate. Here, we analyze Particle Number Size Distributions (PNSD) collected during a year (2015) across four coastal and inland Antarctic research bases (Halley, Marambio, Concordia/Dome C and King Sejong).

We find that the four Antarctic locations have striking differences in PNSD, stressing multiple aerosol sources and processes likely exist. We utilise k-means cluster analysis to separate the PNSD data into six main categories. Nucleation and Bursting PNSDs occur 28-48% of the time between sites, most commonly at coastal sites Marambio and King Sejong where air masses mostly come from the west and travel over extensive regions of sea ice, marginal ice, and open ocean, and likely arise from new particle formation. Aitken high, Aitken low, and bimodal PNSDs occur 37-68% of the time, most commonly at Concordia/Dome C on the Antarctic Plateau, and likely arise from atmospheric transport and aging from aerosol originating likely in both coastal boundary layer and free troposphere. Pristine PNSDs with low aerosol concentrations occur 12-45% of the time, most common at Halley located at low altitudes and far from the coastal melting ice, and influenced by air masses from the west.

The Antarctic Atmospheric circulation has a strong control on the air mass origin type. Most of the time Marambio and King Sejong stations are affected by Easterly air masses, whereas Halley gets air masses mainly from the Weddell sea marginal and consolidated pack ice. Not only the sea spray primary aerosols and gas to particle secondary aerosols sources, but also the different air masses impacting the research stations should be kept in mind when deliberating upon different aerosol precursors sources across research stations.

We provide evidence that both primary and secondary components from pelagic and sympagic regions strongly contribute to the annual seasonal cycle of Antarctic aerosols which add insight on the possible sources of aerosol production/activity in



the whole Antarctic region. Our simultaneous aerosol measurements stress the importance of the variation in atmospheric biogeochemistry across the Antarctic region.

80 **Introduction**

The pristine region of the Southern Ocean (SO) plays a major role in modulating Earth's climate (Carslaw et al., 2013), and natural aerosols are one of the greatest sources of uncertainty in estimates of global radiative forcing (Reddington et al., 2017). This uncertainty becomes greater in polar regions (Carslaw et al., 2013).
85 Aerosols modulate the climate both directly, by absorbing and reflecting radiation, and indirectly, by acting as cloud condensation nuclei (CCN), modulating cloud properties. The surface of the SO near the Antarctic continent goes through an annual freezing cycle; this large frozen area harbours one of the globes largest ecosystems providing a stable habitat for diverse microbial assemblages (Arrigo et al., 2009; 2015). Understanding these processes is key in polar environments where
90 warming processes are rapidly affecting delicate ecosystems (Clem et al., 2020). For example, the Antarctic Peninsula has shown some of the largest increases in near-surface air temperature measured globally across the last 50 years (Turner et al., 2005). Study of the Antarctic environment can also provide an insight into natural
95 preindustrial aerosol processes, and allows us to further our understanding of the preindustrial baseline (Hamilton et al., 2014).

The role of aerosols in the Antarctic is poorly understood as their sources are many and varied in a relatively understudied region. Emissions from the Southern Ocean and the Antarctic region are characterized by multiple environmental systems
100 including open ocean water, sea ice regions, and land, snow covered and snow-free. These regions are being affected by our changing climate (Chen et al., 2009). It has been long known that the seasonal cycle of Antarctic particle number concentrations has a strong seasonal cycle (Shaw 1988), leading to the inference that most of the Antarctic aerosol concentrations is linked with biological processes occurring in the
105 surrounding oceans. It has been proposed that a large "pulse" over summer months arises from the upper Antarctic plateau (Ito et al., 1993; James, 1989), although particle number concentrations are much higher in coastal Antarctica. In other words, it is still debatable if the aerosols originate in the upper troposphere, being



110 transported by the Antarctic drainage flow (James, 1989) to the coast by katabatic
winds (Ito, 1993; Koponen et al., 2002; Fiebig et al., 2014; Hara et al., 2011;
Järvinen et al., 2013; Humphries et al., 2015) or the marine pelagic (ice-free) and
sympagic (ice-containing) boundary layer are a source of ultrafine particles (Herenz
et al., 2019; Weller et al., 2011, 2015, 2018; Dall'Osto et al. 2017; Heintzenberg et
al., 2000, 2023).

115 The Antarctic aerosol summer maximum concentrations (mainly ultrafine particles,
<100 nm) may be largely explained by new particle formation (NPF) events, as
reviewed by Kerminen et al. (2018). Super-micrometre aerosols (>1 µm) will mostly
arise from primary sea spray (O'Dowd et al., 1997a, 1997b; Rankin and Wolff, 2003).
The accumulation mode (100 nm – 1 µm) is a complex intermediary region with both
120 primary and secondary sources related to their multitude of sources and long
atmospheric lifetimes (Fossum et al., 2018; Gras and Keywood, 2017). The relative
importance of these sources undergoes seasonal cycles related to meteorology and
biological productivity.

The roles of secondary aerosols produced from biogenic sulfur mainly derived from
125 the atmospheric oxidation of dimethylsulfide (DMS, a trace gas produced by marine
plankton) and primary sea-spray aerosols in regulating cloudiness above the
Southern Ocean is still a matter of debate (Meskhidze et al., 2006; Korhonen 2008,
Asmi et al., 2010; Quin and Bates, 2011, Fossum 2018, Lachlan-Cope et al., 2020).
The seasonal cycle of primary and secondary aerosol emissions from the SO affect
130 also light scattering by aerosols over all Antarctica, including the upper plateau
(Virkkula et al., 2022). A recent intensification in Antarctic aerosol measurement field
campaigns is revealing that aerosol chemistry in the higher latitudes of Antarctica
can be much more complex than two broad natural sources governing the aerosol
populations: sea spray (primary, mostly composed of sea salt) and non-sea salt
135 sulfate (nssSO₄²⁻; secondary). For example, Paglione et al. (2023) stressed that
various - not yet fully elucidated - sources and aerosol processes are controlling the
Antarctic aerosol primary and secondary population, with the emissions from
sympagic and pelagic ecosystems affecting the variability of submicron aerosol
composition both in maritime areas as in inner Antarctic regions.



140 McCoy et al. (2015) suggested that primary marine organic ultrafine aerosols are
important in the SO region. Saliba et al. (2021) found that the large total organic
fraction of particles $<0.1 \mu\text{m}$ diameter may have important implications for CCN
number concentrations and indirect radiative forcing over the Southern Ocean.
Recently, Humphries et al., (2021) identified three main aerosol sources in the
145 Southern Ocean: northern (40-45 S), mid-latitude (45-65 S) and Southern sector (65-
70 S), with different mixture of continental and anthropogenic, primary and
secondary aerosols depending on the studied region.

Recently, several long-term measurements (in the order of a year or longer) of
aerosol particle number size distributions (PNSD) at a high time resolution allow
150 investigation of the aerosol sources around the Antarctic continent. The PNSD is
typically measured from $\sim 10 - 1,000 \text{ nm}$, and in Antarctica is usually comprised of
particles from secondary (NPF) and primary (blowing snow - BS, Sea Spray
Aerosols - SSA) sources.

At King Sejong Station on the Antarctic Peninsula, (Kim et al., 2017; Park et al.,
155 2023; Kim et al., 2019), Halley on the mainland coast (Lachlan-Cope et al., 2020)
and Concordia/Dome C in the centre of the continent (Järvinen et al., 2013), PNSD
measurements indicated NPF as a summertime and wintertime phenomenon. At
Concordia/Dome C weak and rare but real NPF has been observed even in June,
the darkest time of the year (Järvinen et al., 2013). Particle counts and CCN
160 numbers at Macquarie Island and throughout the Southern Ocean undergo a
summertime maximum (Humphries et al., 2023). The CCN concentration at the onset
of NPF showed an average instantaneous increase of 44% or 11% across the whole
period compared with the background concentration (Kim et al., 2019; Park et al.,
2023). NPF therefore seems to modulate particle and CCN counts in the Antarctic.

165 At Halley, NPF events were shown to arise both from the sea ice marginal zone and
the Antarctic plateau, indicating a marine and free tropospheric source (Lachlan-
Cope et al., 2020). NPF events at King Sejong Station were found more frequently
associated with air masses originating from the Bellingshausen Sea than those from
the Weddell Sea, with a fraction of events being associated with sea ice (Park et al.
170 2023). This suggests the phytoplankton composition of the Bellingshausen Sea may
be a source of NPF precursors (Jang et al., 2019). In Marambio, Quéléver et al.,



(2022) reported important observations of neutral and charged aerosol precursor molecules and chemical cluster composition (qualitatively and quantitatively) - as well as air ions and aerosol particle number concentrations and size distributions -
175 linked with local fauna (mainly penguins), further away from the island; and possibly to the metabolic activity of plankton and accumulation of pre- cursors (e.g., proteins) in the melting sea ice.

Hara et al. (2021) hypothesized that NPF mainly occurred in the Antarctic free troposphere during spring and fall, and in both the free troposphere and boundary
180 layer during summer, based on aerosol number size distributions and their effect on cloud properties observed at Syowa Station. Concordia/Dome C 's observations reported the background particle number size distribution (PNSD) had its largest mode below 30 nm, suggesting these particles were produced in the upper atmosphere before entering continental Antarctica (Järvinen et al., 2013). However,
185 also ground-level particle formation takes place on the upper plateau. Chen et al. (2017) reported NPF events that were observed at Concordia/Dome C by using a combination of an Air Ion Spectrometer (AIS) and a Differential Mobility Particle Sizer (DMPS). In several events particle formation and growth started from the cluster ion size range of 0.9 – 1.9 nm which means that in these cases the formation took place
190 at the ground level. But the compounds, mainly sulphuric acid that are needed for the NPF and growth are not emitted from the upper plateau, their sources are far away. NPF in Antarctica is therefore dependent on biogenic emissions from the ice-covered and ice-free regions of the ocean, with NPF occurring both at ground-level and in the colder upper atmosphere where particle formation rates can proceed more
195 rapidly.

Previous analyses of PNSD at Halley using k-means cluster analysis has shown that wintertime PNSD was characterised by extremely low particle concentrations, with a bimodal size distribution appearing with a blowing snow or sea spray origin (Lachlan-Cope et al., 2020). The Antarctic wintertime at this site is therefore mostly devoid of
200 secondary aerosol sources. NMR analyses of ambient aerosol samples show that aerosols arising from the ice-free Southern Ocean are rich in lipids and sugars, aerosols arising from the ice-covered Weddel sea are rich in methanesulphonic acid and amines, and aerosols arising from coastal areas are rich in sugars associated



with plant vegetation (Decesari et al., 2020). The primary aerosol sources are
205 therefore many and varied across Antarctica.

Here, we apply k-means cluster analysis to simultaneous measurements in the year
2015 at four Antarctic research sites, extending the study of Lachlan-Cope et al.,
(2020). We also compare the yearly data with field studies, including the PEGASO
cruise in 2015 (Dall’Osto et al., 2017a, 2019b; Rinaldi et al., 2019; Decesari et al.,
210 2020) and the continental Antarctic site Kohlen (Weller et al., 2018). We show a
prevalence of new particle formation at the coastal sites, and associate this new
particle formation with air masses flowing over regions of sea ice and ocean. At the
more southerly and inland sites, secondary particles dominate the particle number
concentrations, while air masses primarily travel over regions of land. Ambiguity
215 remains in this analysis, as some PNSD clusters likely contains a substantial
contribution from primary and secondary processes. Nonetheless, we provide further
evidence for the roles of emissions from sympagic and pelagic ocean regions in new
particle formation, and highlight the many and varied sources of particles across
Antarctica.

220 **2 Methodology**

2.1 Sampling sites and measurements

Simultaneous PNSD measurements at four sites across Antarctica were collected for
analysis. Their locations are stated in Table 1, and shown in Figure 1. Data coverage
shown in Figure S1. PNSD measurements were aggregated to 1 hour for this study.

225 The South Korean King Sejong Station, the highest latitude site, is located in the
Antarctic Peninsula. The PNSD from 10 to 300 nm were measured every 3 min with
a mobility particle size spectrometer (MPSS) consisting of a differential mobility
analyzer (DMA; HCT Inc., LDMA 4210) and a CPC (TSI 3772). Details of the site can
be found in (Kim et al., 2017, 2019, Park et al., 2023).

230 The Argentinian Marambio Station is located in the Antarctic Peninsula,
approximately 3 km from the coast. The PNSD from 12 – 800 nm were measured
every 6 min with a differential MPSS (Asmi et al., 2010; Quelever et al., 2022).



The French & Italian operated Concordia/Dome C station is operated on the East Antarctic Plateau at an elevation >3000 m a.s.l, and 900 km from the nearest coast.
235 The Concordia/Dome C sampling site is located 1 km southwest of Concordia/Dome C's main building. The PNSD from 10 – 620 nm were measured every 10 min with a differential MPSS system (Järvinen et al., 2013).

The British Halley VI station is located in coastal mainland Antarctica on the floating Brunt Ice Shelf ~ 20 km from the coast of the Weddell Sea. The The Clean Air Sector Laboratory where PNSD measurements are taken is located 1 km south-east of the station. The PNSD from 6 to 209 nm is measured every 1 min using a TSI Inc. MPSS, comprising an Electrostatic Classifier (model 3082), a Condensation Particle Counter (CPC; model 3775) and a long Differential Mobility Analyser (DMA; model 3081) (Lachlan-Cope et al., 2020).
240

245 **2.2 Data processing**

k-means Cluster Analysis was applied to the PNSD data to apportion the PNSDs according to their shape (Beddows et al., 2009), and is routinely applied in pristine environments to PNSD data (Dall'Osto et al., 2017b, 2019b; Lachlan-Cope et al., 2020). k-means apportions data into k clusters such as the sum of squares of
250 distances of data to the cluster centre is minimised. In the case of MPSS data, this produces well-separated clusters (Beddows et al., 2009). First, data were normalised so the Euclidian length of each PNSD was 1, so the clustering is done solely on the merit of the shape of the PNSDs. Here, a degree of distance between clusters was achieved with 16 MPSS clusters. These were assigned into 6 categories typical of
255 Antarctic PNSDs (Lachlan-Cope et al., 2020).

The condensation sink (CS , s^{-1}) represents the rate at which a vapour phase molecule will collide with pre-existing particle surface, and was calculated from the PNSD data as follows (Kulmala et al., 2012):

$$CS = 2\pi D \sum_{d_p} \beta_{m,d_p} d_p N_{d_p} \quad (1)$$

260 Here, we presume the vapour phase molecule in question is sulphuric acid.



2.3 Air mass trajectories

Air mass back trajectories were calculated using the HYSPLIT4 (Hybrid Single Particle Lagrangian Integrated Trajectory) trajectory model (Draxler and Rolph, 2010) arriving at the sampling site every one hour. Each back-trajectory data point
265 was assigned to a surface-type (land, sea, ice, or snow over land. A cell is considered ice-covered if more than 40% of the cell is covered with ice) on a 24 km grid from the daily Interactive Multisensor Snow and Ice Mapping System (IMS) (Ice, 2008). To investigate air masses concurrent with high particle count, these 72-hour back-trajectories were gridded to 1x1 grid cells of 1 degree each, and linked back to
270 the total integrated particle number concentration from the PNSD measurements by the following equation:

$$\ln(\bar{c}_{ij}) = \frac{1}{\sum_{k=1}^N \tau_{ijk}} \sum_{k=1}^N \ln(c_k) \tau_{ijk} \quad (2)$$

Where \bar{c}_{ij} is the concentrated weighted trajectory (CWT) at cell i, j , N is the total number of trajectories, c_k is the value of particle number (N) associated with the
275 arrival of trajectory k , and τ_{ijk} is the residence time of trajectory k in grid cell i, j . \bar{c}_{ij} therefore describes the source strength of condensable vapour that drives particle growth from any particular grid cell (Hsu et al., 2003; Lupu and Maenhaut, 2002). This was done using the `trajLevel` function in the `Openair` package in R 3.6.3.

3 Results

280 3.1 Trends in aerosol PNSDs

The mean PNSD for the measured periods are shown in Figure 2a. PNSDs at the two Antarctic Peninsula sites, Marambio and King Sejong show large nucleation modes. Aitken mode peaks are present at all sites with maximum concentrations between 30 and 50 nm. Accumulation mode peaks are present at all sites with
285 maximum concentrations >100 nm. The prominent nucleation modes at Marambio and King Sejong are also visible in the daily contour plots, with the visible signature of a new nucleation mode in the late and early afternoons (local times) at the two sites, respectively (Figure S3). Total average particle counts are highest at King



290 Sejong & Marambio, (312 ± 601 and 270 ± 541 cm^{-3}), particle counts at Halley are lower (223 ± 245 cm^{-3}), while those at Concordia/Dome C are 44 ± 67 cm^{-3} .

The monthly variation in total particle number (N_{tot}) is similar between all sites, highest in the austral summer, with minimum values in July & August. N_{tot} at Concordia/Dome C is substantially lower in near all months compared to all other sites, with the monthly average only exceeding 100 cm^{-3} in the Austral Summer months (Nov, Dec). Relative contributions of the modes <30 nm, 30 - 100 nm, and >100 nm to N_{tot} at each site is shown in Figure 2d. The relative contribution of <30 nm particles is highest at Marambio and King Sejong, exceeding 50% of the total N_{tot} at Marambio, consistent with the prominence of the presence of the nucleation mode (Fig. 2a). The contribution of <30 nm particles to total N_{tot} is lowest at Halley, where 295 $\sim 50\%$ of the N_{tot} comes from the mode 30 - 100 nm, and $\sim 30\%$ from the mode >100 nm. At Concordia/Dome C, $\sim 65\%$ of N_{tot} comes from the mode 30 - 100 nm, with small contributions from particles above or below this size range. 300

3.2 Cluster analysis

305 3.2.1 Categorising PNSD K-means clusters

K-means cluster analysis was used to partition the PNSD data into days with similarly shaped PNSD data. In k-means cluster analysis, starting with a higher number of clusters and then merging them based on similarity can enhance the separation and interpretability of the final clusters by capturing finer details. These 16 310 daily K-means clusters (Figure S2, referred to onwards as the initial PNSD clusters) were therefore aggregated into 6 daily categories typical of Antarctic PNSD data (referred to as simply the PNSD clusters) for further analysis based on the shape of the PNSD and their temporal variation (Figure 3a and 3b). These are Nucleation, Bursting, Aitken low, Aitken high, Bimodal, and Pristine, following previous 315 classification described in previous studies (Dall'Osto et al., 2017b; Dall'Osto et al., 2019, Lachlan-Cope et al., 2020). The diurnal cycle of the PNSD belonging to each of the initial 16 K-means clusters at each of these sites is shown in Figure S4, while



the diurnal cycle of the merged clusters is shown in Figure S5, separated by site, and the PNSD per cluster separate by season is shown in Figure S6.

320 Two clusters relate to NPF: Nucleation (mean particle count $502 \pm 1087 \text{ cm}^{-3}$) has a mean PNSD with a peak at 12 nm averaged between all sites. This corresponds to fresh new particles generated during NPF events and will correspond to days of measurements dominated by a signature of new particles appearing in the PNSD, typically with signs of growth. Bursting (mean particle count $177 \pm 350 \text{ cm}^{-3}$) has a
325 mean PNSD with a peak at 22 nm averaged between all sites, and typically corresponds to days where new particles form, either fail to grow, are lost to coagulation, or are diluted and lost at the receptor site. These likely still do correspond to secondary formation processes. We presume here that there is no primary contribution to these PNSDs

330 Aitken is the most common PNSD category separated into Aitken high (mean particle count $401.6 \pm 45.5 \text{ cm}^{-3}$), and Aitken low (mean particle count $208.8 \pm 216.7 \text{ cm}^{-3}$). The mean PNSD shows peak concentrations at about 20-35 nm and 35-55 nm respectively. These two clusters are separated based on their aerosol total concentrations. The name of this category emerges from growing ultrafine aerosol
335 resulting from the processing of local and regional marine aerosols, a phenomenon previously described to occur mainly in summer (Dall'Osto et al., 2017b).

Pristine (mean particle count $142 \pm 134 \text{ cm}^{-3}$) has a mean PNSD with a peak at 88 nm. The name of this category emerges from the extremely low "pristine" particle number concentrations. The three K-means clusters belonging to this categories
340 have some specific aerosol modes, peaking at 65 nm, 85 nm and a much larger accumulation mode at 160 nm (Figure S2) likely associated at pristine conditions with high loadings of blowing snow, as previously discussed in Lachlan-Cope et al. (2020).

Bimodal (mean particle count $107 \pm 133 \text{ cm}^{-3}$) has two peaks in the PNSD at 39 and
345 113 nm. Both are characterised by low particle counts. The name of this category is associated with the bimodal PNSD. The two initial clusters differ slightly because of the Hoppel minimum at 55nm and 75nm, respectively, possibly indicating different chemistry and particle origin.



The condensation sink represents the main loss process for many low-volatility vapours which contribute to new particle formation. The condensation sinks for the Bursting K-means cluster is lowest ($2.3 \cdot 10^{-4} \text{ s}^{-1}$), followed by Bimodal ($2.4 \cdot 10^{-4} \text{ s}^{-1}$), Pristine ($3.4 \cdot 10^{-4} \text{ s}^{-1}$), Nucleation ($3.7 \cdot 10^{-4} \text{ s}^{-1}$), and Aitken low ($3.4 \cdot 10^{-4} \text{ s}^{-1}$), and Aitken high ($4.0 \cdot 10^{-4} \text{ s}^{-1}$). Particle counts change by around 1 order of magnitude between sites, but the shapes of the PNSD are similar (Figure S2, S5). All Nucleation PNSDs show formation of and growth of particles at midday and afternoon times (local time), while Bursting show particles at or near the smallest sizes, sometimes with indication of particle growth.

3.2.2 Trends in PNSD K-means clusters

The frequency of occurrence of these different PNSD clusters can indicate the dominant sources of aerosol particles at each of these time periods. All sites have a large contribution from Aitken low and Aitken high PNSD clusters, with 37% of PNSDs falling into these categories across all four sites. Marambio is also dominated by PNSD clusters falling into the Nucleation and Bursting category, (25% and 23% of PNSDs, respectively). There is a smaller contribution of Nucleation and Bursting to the PNSDs at King Sejong (8% and 20% respectively). These PNSD clusters contribute little at Halley (3% and 3%, respectively), and at Concordia/Dome C (2% and 5%, respectively). Halley instead sees a large contribution of Pristine PNSDs (45% of PNSDs), and Concordia/Dome C sees a large contribution of Bimodal PNSDs (34% of PNSDs) (Figure 3a).

The seasonal evolution of these K-means clusters is shown in Figure 3c. At Marambio, the contribution of Nucleation and Bursting PNSDs occurs in nearly all months. At King Sejong, Nucleation and Bursting PNSDs are most frequent in the spring and autumn months, while Pristine air masses are most common in the Austral winter. At Halley, Aitken PNSDs dominate the warmer months, while Pristine air masses dominate the colder winter months. At Concordia/Dome C, where data are available, Bimodal PNSDs dominate the winter, while Aitken dominates the warmer months. There is a substantial contribution of Nucleation and Bursting in the month of September also. When all sites are averaged, a clear seasonal cycle is



380 seen, with pristine and bimodal PNSDs dominating in the coldest months, and a
substantial contribution of Aitken in the warmer months. Nucleation is slightly higher
in the warmer months (particularly January through March), while bursting PNSDs
are higher outside of these months.

3.3 Air mass analysis

385 72 hour HYSPLIT back trajectories arriving at the four different measurement sites
for every hour with PNSD data were calculated. The amount of time each of these air
masses spent flowing over land, open ocean, marginal ice, or sea ice per K-means
cluster across all sites is plotted in Figure 4a, and per site is plotted in Figure 4b. On
average, the air masses arriving at the sites had flown over mostly the land of the
390 Antarctic continent (54%), with a 24% contribution from sea ice, 15% contribution
from open water, and a small (6%) contribution from marginal ice. Nucleation &
Bursting PNSDs occur when air masses have travelled under substantially less land
and over more sea ice, marginal ice, and ocean than average (40%, 8%, and 26% of
air mass hours for Nucleation, and 34%, 10%, and 25% of air mass hours for
395 Bursting, respectively). At Marambio, the main contribution is air masses arising from
sea-ice regions (50%) which is highest for Bimodal PNSDs (76%). The contribution
of open water to Aitken, Bursting & Nucleation is higher than average (23%), while
the contribution of sea ice to these air masses is lower (44%). At King Sejong, air
masses spend the majority of their time travelling over regions of open water (41%)
400 and sea ice (33%). The contribution of open water is higher for bimodal (51%) and
Aitken PNSDs (58%). At Halley, air masses spend the majority of their time flowing
over land regions (79%), with a small contribution from sea ice (15%). The
contribution of sea ice to Nucleation PNSDs is substantially higher (30%). At
Concordia/Dome C, air masses arriving at the receptor site mostly flow over land
405 (99%). The contribution of sea ice, marginal ice, and open water are higher for
bursting PNSDs (9% in total).

Our CWT (concentrated weighted trajectory) analysis grids back trajectories to 1x1
degree squares and weighs each segment of the back trajectory with the
corresponding N_{tot} observed upon the air mass's arrival, performed individually for
410 each PNSD cluster. These are plotted in Figure 5. A map highlighting source regions
for N_{tot} unseparated by cluster per site is shown in Figure S8. The CWTs separated



by cluster and site is shown in Figure S9. Mean heights of these trajectories are shown in Figure S10.

The sources of particles by number (or, N_{tot}) across all PNSD data at the two
415 Antarctic Peninsula sites Marambio and King Sejong are to the west of the peninsula, across the iced and open water regions of the Bellingshausen Sea and to a lesser extent the Weddell sea. Those at Halley are concentrated at the coastal and land-based regions, with some influence from the Weddell sea, while the highest aerosol concentrations at Concordia/Dome C arise from mostly land regions, with
420 some trajectories extending past the southern tip of the continent over ocean regions (Figure S8).

Air masses arriving at the Antarctic sites corresponding to Nucleation & Bursting K-means clusters pass mostly over the Bellingshausen sea at Marambio and King Sejong. Air masses passing over the regions just west of the peninsula have a high
425 source contribution to high number concentrations of particles especially, as do the more northerly regions off the southern tip of south America. At Halley, these PNSD clusters are mostly associated with coastal regions, consistent with the higher contribution of sea ice. The source contributions at Concordia/Dome C correspond to a small number of trajectories. All trajectories corresponding to Nucleation PNSDs
430 have a lower-than-average trajectory height (Figure S10).

Aitken PNSDs have strong source contributions from the entire Bellingshausen sea region at Marambio and King Sejong. At Halley, there is a strong contribution from land mass regions, while at Concordia/Dome C, land and regions mostly contribute to this PNSD. Bimodal and Pristine air masses at Marambio and King Sejong have
435 strong source contributions from the iced regions either side of the Antarctic peninsula, covering the Weddel and Bellingshausen seas. This is consistent with the higher contribution from sea-ice regions to these K-means clusters. At Halley, the Bimodal PNSDs arise when air masses flow over coastal and land-based regions, while Pristine PNSDs, which are extremely frequent at this site, arise largely from the
440 Antarctic continent itself. At Concordia/Dome C, there is a strong source contribution to Bimodal & Pristine PNSDs from air masses flowing over the coastal region of southern Antarctica, as well as some land regions. Trajectories corresponding to Pristine PNSDs have, on average, a higher trajectory height than average.



3.4 Intercomparison with other existing data across the year 2015

445 3.4.1 PEGASO cruise

The PEGASO (Plankton-derived Emissions of trace Gases and Aerosols in the Southern Ocean) cruise was conducted on board the RV Hesperides in the regions of Antarctic Peninsula, South Orkney and South Georgia Islands from 2 January to 11 February 2015. It was found that the microbiota of sea ice and the sea ice-influenced ocean can be a source of atmospheric primary and secondary organic nitrogen (ON), specifically low molecular weight alkylamines (Dall'Osto et al., 2017; 2019). Other follow up studies also claim that the potential impact of the sea ice (sympagic) planktonic ecosystem on aerosol composition were overlooked in past studies, and multiple eco-regions act as distinct aerosol sources around Antarctica (Decesari et al., 2020; Rinaldi et al., 2020).

Figure 6a shows the intercomparison of MPSS PNSDs for the PEGASO cruise. These are separated into times when the air masses flowed over the Pacific ocean, and over the Weddel sea. This is compared with stations used for this study where overlapping data are available (Marambio, King Sejong, and Halley). Air masses from the Southern Pacific Ocean with anthropogenic and terrestrial influence from Patagonia are likely responsible for the higher Aitken mode seen for the "Pacific" PNSD during the PEGASO cruise. By contrast, cruise measurements influenced by the Weddel sea show a PNSD similar to the three stations intercompared, suggesting little anthropogenic influence of the latter. Dall'Osto et al., (2017) showed that sea ice regions are a strong source of sub-3 nm particles in Antarctica relative to open water regions. The present study, considering a much broader dataset, also shows that the Open Water (OW) regions sampled at Marambio and at King Sejong stations are also associated with enhanced NPF.

470 3.4.2 Kohnen station

Weller et al., (2018) reported PNSDs and conducted bulk and size-segregated aerosol sampling during two summer campaigns in January 2015 and January 2016 at the continental Antarctic station Kohnen (Dronning Maud Land). The transport of aerosols was associated with two main weather conditions: (1) the sporadic impact



475 of cyclones causing high loadings of marine aerosol concentrations and NPF and (2)
clear sky conditions causing long range transport of aged aerosols. Figure 6b shows
similar aerosol PNSDs among Kohnen, Halley and King Sejong stations for the same
sampling period in 2015. By contrast, much higher concentrations of ultrafine
particles - likely due to NPF - were seen occurring at Marambio. This may be a
480 combination of local sources (nearby penguin colonies) and melting sea ice during
the summer period, given Marambio is the station among all closest to marginal sea
ice zones (Quelever et al., 2022).

4 Discussion

4.1 Possible primary sources

485 Of our six aerosol categories, nucleation and bursting are related to secondary
aerosols, while the two Aitken K-means clusters likely have significant contributions
from primary and secondary processes (Figure 2a), although the latter may
dominate. Bimodal PNSDs are likely associated with aged and processed marine
aerosols (the Hoppel minimum mode is seen at about 70 nm, Hoppel et al., 1994).
490 We cannot apportion primary aerosols from our PNSD measurements without any
chemical composition information, but can hypothesise some. Sea salt aerosol
particles are formed from open ocean regions when sea spray is produced by wave
breaking and bubble bursting generating film and jet drops (De Leeuw et al., 2011).
Sea salt aerosol is also formed from blowing snow above sea ice (Frey et al., 2020).
495 These mechanisms are thought to contribute equally to sea salt aerosol loads
(Legrand et al., 2016), while blowing snow over land is a source from continental
Antarctica (Giordano et al., 2018).

In the periods where NPF is negligible, there are still other primary aerosol sources.
We show that pristine and bimodal PNSD clusters dominate through the winter
500 (Figure 3c, S6). It is therefore important to characterize these pristine conditions. The
three K-means clusters of the pristine categories have similar low particle number
concentrations, but one of the three has a distinct PNSD. The cluster (pristine_160)
seen with a bimodal PNSD (75 and 160 nm, respectively), was strongly associated
with high wind speed and possibly associated with blowing snow and sea spray sea
505 salt, dominating the winter aerosol population (Lachlan-Cope et al., 2020). When the



four stations are compared in this study, it can clearly be seen that Halley has the most frequent pristine conditions (45%, relative to the 12-20% of the other three), also relative to Concordia/Dome C where we propose that free troposphere transport and aged aerosols populate the PNSD with Aitken modes and bimodal PNSDs.

510 The pristine initial PNSD cluster with a strong peak at 160nm (table S1) is seen mainly at Halley (12%) relative to the other stations (2-3%). A study by Yang et al. (2019) proposes a source for ultrafine sea salt aerosol particles from blowing snow, dependent on snow salinity. This mechanism could account for the small particles seen during Antarctic winter at coastal stations (Giordano et al., 2018; Frey et al.,
515 2020). Recently, similar PNSD were reported by Gong et al., (2023) in the central Arctic over an entire year from September 2019 to October 2020 during the Multidisciplinary drifting Observatory for the Study of Arctic Climate (MOSAIC) expedition, showing that blowing snow was observed more than 20% of the time from November to April. The sublimation of blowing snow generates high
520 concentrations of fine-mode sea salt aerosol (diameter below 300 nm), enhancing cloud condensation nuclei concentrations up to tenfold above background levels (Gong et al., 2023).

Primary marine organic aerosol in the submicron regime is likely produced separately from sea salt (Gantt and Meskhidze, 2013). At the coastal sites of
525 Marambio and Halley, Bimodal and Pristine PNSDs with the highest particle number concentration arise mostly from the Bellingshausen Sea, where DMS(P)-rich phytoplankton concentrations are very high. A dominant biological oceanic mechanism of primary particle origin at these sites is therefore likely. Given the vastly different source characteristics between these sites, it is likely that the
530 dominant mechanisms of origin of these primary particles, and therefore our bimodal and pristine clusters also differ between sites, but it is clear that primary emissions dominate the PNSD in the Antarctic winter.

4.2 New particle formation and possible secondary sources

We identify two PNSD clusters which we classify as arising from secondary
535 processes, these are Nucleation and Bursting PNSDs. The Aitken PNSD clusters cannot be definitively said to contain solely particles from secondary processes,



although they have similar source regions (Figure S5) and could consist of grown particles formed either elsewhere in the boundary layer or in the free troposphere, with average growth rates around $\sim 0.1 - 1 \text{ nm h}^{-1}$ (Brean et al., 2021; Järvinen et al., 540 2013; Jokinen et al., 2018; Kim et al., 2019), particles formed through NPF would grow to the sizes observed in this PNSD cluster on the order of ~ 2 days. The contribution of Aitken PNSDs is greatest outside of the winter months (Figure S7). However, below, we will purely discuss the contribution of the Bursting and Nucleation PNSDs.

545 NPF in Antarctica is a summertime phenomenon largely responsible for the seasonal cycle in particle number concentrations (Figure 2c). This cycle has been observed at at King Sejong Station (Kim et al., 2017; Park et al., 2023; Kim et al., 2019), Halley (Lachlan-Cope et al., 2020) and Concordia/Dome C (Järvinen et al., 2013; Chen et al., 2017). This corresponds with periods of high biological and photochemical 550 activity (Jang et al., 2019; Kim et al., 2019). These observations are consistent with our observed higher frequency of Nucleation PNSD clusters in January through March (Figure 3c, S6). However, we consistently observe Nucleation and Bursting PNSDs year-round, even at sites where manual inspection of these PNSDs has found little to no NPF in the winter seasons (Kim et al., 2019).

555 We frequently observe PNSDs with a large nucleation mode in the Austral summer (Figure S7). NPF is mainly influenced by the source rates of vapours (DMS, VOC, base, and iodine emissions, OH \cdot and O $_3$ production rates), loss rates of vapours and new particles (CS), ion pair production rates, and temperature (Lee et al., 2019). Vapour source rates will be lowest in winter, however, ion pair production from 560 cosmic rays is likely constant, while loss rates of vapours and temperatures have a wintertime maximum. Some number of particles may therefore form and be identified by Cluster analysis, even when they do not give the visual signature of an NPF event.

Our analyses show that coastal Antarctic sites nearest to the melting sea ice are 565 most influenced by NPF (Figure 3c) where a large fraction of the PNSDs are classified as Nucleation and Bursting (48 and 28% at Marambio and King Sejong respectively). Further, we show that NPF is frequent when air masses flow over the ice-influenced oceanic Antarctic regions (Figure 4,5). NPF events have been shown



to be frequent and strong at coastal Antarctic sites (Brean et al., 2021; Jokinen et al.,
570 2018), but most rapid at those nearest to melting ice (Brean et al., 2021) as well as
near local sources associated with penguin colonies (Quelever et al., 2022). Recent
observations shows that this does not extend across the whole of the southern
ocean (Baccarini et al., 2021). Our PNSD cluster analysis is consistent with this.
Melting sea is therefore a likely source of NPF precursors in the Antarctic Peninsula
575 region.

High aerosol number concentrations arising from the Bellingshausen sea is
consistent with a previous analysis of NPF at King Sejong (Jang et al., 2019).
Bursting and nucleation aerosol categories in particular exhibit high number
concentrations when air masses pass over the regions just west of the peninsula
580 (Figure 5). These regions have been shown to be rich in alkylamines (Dall'Osto et
al., 2019a) that lead to rapid and efficient particle formation (Brean et al., 2021).
There is evidence that these melting sea-ice regions are sources of numerous NPF
precursors (Atkinson et al., 2012; Dall'Osto et al., 2017a, 2019a). This is also
consistent in the sympagic Arctic environment (Dall'Osto et al., 2017b, 2018).
585 Consistent with this, the results of our K-means cluster analysis show that the sites
with the highest exposure to air masses that pass over regions of sea ice and
marginal ice have by far the greatest contribution from nucleation and bursting PNSD
types (Figure 2, 4). The sites where air masses primarily travel over snow-covered
land regions have, by contrast, very little contribution of nucleation and bursting
590 (Figure 4a).

The role of new particles formed in the free-troposphere and transported down to our
receptor sites is unknown, but likely. Particle formation processes are highly efficient
in the free troposphere given the lower temperatures and higher ion pair production
rates. A wider number of potential nucleation mechanisms are therefore likely (Kirkby
595 et al., 2011; Wang et al., 2022). Modelling studies predict a substantial fraction of
CCN in all seasons (Korhonen et al., 2008). These particles, if arriving at the
receptor site long enough after formation, will contribute either to Nucleation,
Bursting, or Aitken PNSDs. While we therefore highlight source regions leading to
boundary layer NPF processes, we cannot state what fraction of PNSDs arise from
600 free tropospheric particle formation processes.



During the austral summer the concentration of DMS in the water of the Southern Ocean is the highest of the planet (Lana et al., 2011), with high fluxes into the atmosphere, potentially producing high concentrations of sulphuric acid and methanesulphonic acid. However, under typical boundary layer conditions the concentration of sulphuric acid is too low to form particles alone, and another molecule, such as ammonia, is required to stabilize the nucleating clusters (Kirby et al., 2011). Jokinen et al. (2018) reported the first molecular characterization of NPF from the Aboa station in Antarctica, showing that new particles are formed via clustering of sulfuric acid and ammonia (Kirby et al., 2011). Sources of ammonia and alkylamines are related to animals, mainly birds and seal colonies and melting sea ice, but the relative importance of each source is unknown (Riddick et al., 2012; Schmale et al., 2013, Brean et al., 2021; Quelever et al., 2022). Iodine oxoacids are also capable of efficiently forming new particles (Baccarini et al., 2020; He et al., 2021; Sipilä et al., 2016), with iodic acid being able to efficiently stabilise clusters of iodic and sulphuric acid, even in the absence of ammonia (He et al., 2023), with modelling studies showing high gas-phase iodine concentrations across Antarctica (Saiz-Lopez et al., 2007). Further, the formation of marine primary aerosol particles and of gas-to-particles precursors is influenced by the uppermost layer of the ocean, the so called sea surface microlayer (SML) (Cunliffe et al., 2013). The SML - with physicochemical characteristics different from those of subsurface waters (SSW) - results in dense and active viral and microbial communities (Vaquer et al., 2021, Heinrichs et al., 2024). The microlayer of the ocean is a source of oxygenated VOCs in the Arctic leading to secondary aerosol formation (Mungall et al., 2017), and it is also likely a source in the Southern Ocean too although no measurements of this type are available.

Therefore, while the limited number of measurement studies implicate sulphuric acid and nitrogenous bases as the drivers of NPF, iodine and VOCs may play a substantial role.

5 Implication and conclusion

To gain insight into the influence of marine Antarctic biogeochemistry on atmospheric aerosol, we report simultaneous aerosol PNSDs collected across an entire year (2015) at four research stations (Marambio, King Sejong, Halley, and



Concordia/Dome C), as well as a brief intercomparison with a cruise around the regions of Antarctic Peninsula, South Orkney, and South Georgia Islands (Dall'Osto et al., 2017) and a field campaign in Kohnen station (Weller et al., 2018). Our study shows that the aerosol PNSDs across the Antarctic have striking differences, confirming that multiple eco-regions, with subsequent atmospheric chemical and physical processes, act as multiple aerosol sources around Antarctica. These analyses suggest that the PNSD of Antarctic sub-micrometre aerosols may have been oversimplified in the past (Ito, 1993) and that complex interactions between multiple ecosystems, coupled with different atmospheric circulation, result in very different PNSDs populating Antarctica. Our knowledge on aerosol sources of primary and secondary origin is limited.

Recently, Brean et al., (2023) emphasized how understanding the geographical variation in surface types across the Arctic is key to understanding secondary aerosol sources, highlighting that particle formation and growth rate vary tremendously likely due to different regions producing different precursors source rates. We argue that the same complexity applies to Antarctica - an ensemble of regions with substantial spatial heterogeneity across marine, terrestrial, and freshwater biomes, with productivity and biodiversity patchiness super-imposed on strong environmental gradients. Antarctica, one of the world's eight major biogeographical realms, is made up almost entirely of one single bioregion - the ice-covered land mass, coastal tundra, and sea ice of the main continent. It contains two additional marine bioregions - the Antarctic Peninsula & Scotia Sea and the Subantarctic Indian Ocean Islands (Chown et al., 2007; Terauds et al., 2012, 2016). A bioregion is smaller in scale than a biogeographical realm but larger than an eco-region or an ecosystem, it allows the integrations of multiple eco-regions, including terrestrial, freshwater and marine into a cohesive system. Whilst these definitions may be challenging in the context of atmospheric biogeochemistry, we argue a better understanding of the interactions between the biosphere and the geosphere are needed to better understand aerosol sources in Antarctica.

Antarctic sea ice covers between 1% (summer) and 5% (winter) of the global ocean. Antarctic terrestrial productivity and biodiversity occur almost exclusively in ice-free areas that cover less than 1% of the continent. In Antarctica the coastline extends for



665 17,968 km and comprises about $34.8\text{-}36.4 \times 10^6$ km² where 80% of this surface is
covered by ice, even in summer (Peck et al., 2018; Ronowicz et al., 2019). Overall,
there is about 390,071 km² of coast shallower than 200 m (Peck et al., 2018).
Antarctic coastal systems harbour a high diversity of marine and terrestrial
ecosystems including Antarctic seaweeds (benthonic macroalgae) and bird colonies
670 (mainly penguins). Antarctic seaweeds (often called macroalgae) are found in
shallow (<200m) coastal, rocky shores and can cover more than 80% of the benthic
surface (Amsler et al., 2005; Wiencke and Amsler, 2012). The Antarctic and Sub-
Antarctic region is home for about half of the total worldwide seabird population
(Otero et al., 2018). Penguins represents a high proportion of the avian biomass, and
675 their fecal material is one of the main source of phosphorus and nitrogen,
representing about 80% of these elements in the Antarctic marine environment.
Seabird colonies also represent a significant source of atmospheric ammonia (NH₃)
in remote maritime systems (Riddick et al., 2012, Schmale et al., 2013). These
emissions are environmentally relevant as they primarily occur as “hot-spots” in
680 otherwise pristine environments.

Figure 7 (a, b) shows a schematic illustration of the sea ice, microbiota, sea-to-air
emissions, and primary and secondary aerosols in Antarctica. The Southern Ocean
is among the largest source of Sea Spray Aerosols (SSA) on our planet Earth.
Current aerosol models have a large uncertainty in the SSA abundance (Lapere et
685 al., 2023) and the relative importance of the sublimation of blowing snow is not yet
quantified (Giordano et al., 2018; Frey et al., 2020). The biogenic organic component
of SSA in Antarctica is thought to be important (Mc Coy et al., 2015) but again not
fully quantified. Sea ice may also modulates SSA production, with potentially
significant climate impacts (Dall’Osto et al., 2022a). Other leached material from
690 Antarctic media including seaweeds and penguin guano may also affect cloud-
relevant aerosol SSA production (Dall’Osto et al., 2022b).

The changes occurring in the Antarctic environment will modify the climate with
feedbacks and exchanges between the biosphere and cryosphere with the
atmosphere. Changes in marine and terrestrial life - including adaptation of
695 ecophysiology, food and nutrient availability - will affect the emissions of primary and
secondary aerosol precursors. Interdisciplinary studies and international cooperation



in Antarctica are reducing the gap in our knowledge of these key environmental factors.

Code and data availability.

700 The code and data used to produce all non-illustrative figures are available from the corresponding authors under reasonable request.

Supplement.

The supplement related to this article is available online at: X

Author contributions.

705 Conceptualization: MDO conceptualized the paper following the study of Lachlan-Cope et al (2020).

Data Curation: EA provided data for Marambio; TLC and AJ provided data for Halley, AL, AV, PA provided data for Concordia/Dome C, and JP and YJY provided data for King Sejong.

710 Software: DCSB and JB.

Formal Analysis: DCSB, JB, MDO.

Funding Acquisition: See acknowledgement.

Methodology: DCBS, JB.

Project Administration: MDO.

715 Resources: See acknowledgement.

Validation: Validated by all co-authors.

Visualization: JB.

Writing: JB, MDO

Review & Editing: all authors.

720

Competing interests.

At least one of the (co-)authors is a member of the editorial board of Atmospheric Chemistry and Physics.

Disclaimer.

725 Publisher's note: Copernicus Publications remains neutral with regard to jurisdictional claims in published maps and institutional affiliations.



Acknowledgements.

This work acknowledges the ‘Severo Ochoa Centre of Excellence’ accreditation
730 (CEX2019-000928-S). The National Centre for Atmospheric Science (NCAS)
Birmingham group is funded by the UK Natural Environment Research Council. The
Antarctic cruise PEGASO was led by Dr. R. Simo (ICM-CSIC). We also thank Miss
Chantal Jackson GEES Drawing Office from the University of Birmingham (UK).

Financial support.

735 The study was supported by the Spanish Ministry of Economy through project PI-ICE
(CTM2017–89117-R) and POLAR- CHANGE (PID2019-110288RB-I00) and the
National Centre for Atmospheric Science funded by the Natural Environment
Research Council. We acknowledge support of the publication fee by the CSIC
Open Access Publication Support Initiative through its Unit of Information Resources
740 for Research (URICI). Additional sources come from Research council of Finland
(335844, 346372). EA, AV and MS were supported by the Academy of Finland
project Antarctic Climate Forcing Aerosol (ACFA) (decision nr. 335845).

745

References

Amsler et al., 2005 C.D. Amsler, K. Iken, J.B. McClintock, M.O. Amsler, K.J. Peters, J.M.
Hubbard, F.B. Furrow, B.J. Baker Comprehensive evaluation of the palatability and chemical
750 defenses of subtidal macroalgae from the Antarctic peninsula *Mar. Ecol. Prog. Ser.*, 294
(2005), pp. 141-159

Arrigo, K. R., Lizotte, M. P., Mock, T. Primary producers and sea ice. *Science* 2009 pp
283–326.

755



Arrigo, K. R.; van Dijken, G. L.; Strong, A. L. Environmental controls of marine productivity hot spots around Antarctica. *J. Geophys. Res. - Oceans* 2015, 120, 5545–5565.

- 760 Asmi, E., Frey, A., Virkkula, A., Ehn, M., Manninen, H. E., Tiimonen, H., Tolonen-Kivimäki, O., Aurela, M., Hillamo, R., and Kulmala, M.: Hygroscopicity and chemical composition of Antarctic sub-micrometre aerosol particles and observations of new particle formation, *Atmos. Chem. Phys.*, 10, 4253–4271, <https://doi.org/10.5194/acp-10-4253-2010>, 2010
- 765 Atkinson, H. M., Huang, R. J., Chance, R., Roscoe, H. K., Hughes, C., Davison, B., Schönhardt, A., Mahajan, A. S., Saiz-Lopez, A., Hoffmann, T. and Liss, P. S.: Iodine emissions from the sea ice of the Weddell Sea, *Atmos. Chem. Phys.*, 12(22), 11229–11244, doi:10.5194/acp-12-11229-2012, 2012.
- 770 Baccarini, A., Karlsson, L., Dommen, J., Duplessis, P., Vüllers, J., Brooks, I. M., Saiz-lopez, A., Salter, M., Tjernström, M., Baltensperger, U., Zieger, P. and Schmale, J.: Frequent new particle formation over the high Arctic pack ice by enhanced iodine emissions, *Nat. Commun.*, (2020), 1–11, doi:10.1038/s41467-020-18551-0, 2020.
- 775 Baccarini, A., Dommen, J., Lehtipalo, K., Henning, S., Modini, R. L., Geysel-Ber, M., Baltensperger, U. and Schmale, J.: Low-Volatility Vapors and New Particle Formation Over the Southern Ocean During the Antarctic Circumnavigation Expedition, *J. Geophys. Reseaerch Atmos.*, (126), 2021.
- 780 Beddows, D. C. S., Dall'Osto, M., Harrison, R. M., Dall'Osto, M., Harrison, R. M., Dall'Osto, M. and Harrison, R. M.: Cluster Analysis of Rural, Urban, and Curbside Atmospheric Particle Size Data, *Environ. Sci. Technol.*, 43(13), 4694–4700, doi:10.1021/es803121t, 2009.
- 785 Brean, J., Dall'Osto, M., Simó, R., Shi, Z., Beddows, D. C. S. and Harrison, R. M.: Open ocean and coastal new particle formation from sulfuric acid and amines around the Antarctic Peninsula, *Nat. Geosci.*, doi:10.1038/s41561-021-00751-y, 2021.
- 790 Brean, J., Beddows, D. C. S., Harrison, R. M., Song, C., Tunved, P., Ström, J., Krejci, R., Freud, E., Massling, A., Skov, H., Asmi, E., Lupi, A., and Dall'Osto, M.: Collective geographical ecoregions and precursor sources driving Arctic new particle formation, *Atmos. Chem. Phys.*, 23, 2183–2198, <https://doi.org/10.5194/acp-23-2183-2023>, 2023.
- 795 Carslaw, K. S., Lee, L. A., Reddington, C. L., Pringle, K. J., Rap, A., Forster, P. M., Mann, G. W., Spracklen, D. V., Woodhouse, M. T., Regayre, L. A. and Pierce, J. R.: Large contribution of natural aerosols to uncertainty in indirect forcing, *Nature*, 503(7474), 67–71, doi:10.1038/nature12674, 2013.
- Clem, K. R., Fogt, R. L., Turner, J., Lintner, B. R., Marshall, G. J., Miller, J. R. and Renwick, J. A.: Record warming at the South Pole during the past three decades, *Nat. Clim. Chang.*, 10(8), 762–770, doi:10.1038/s41558-020-0815-z, 2020.



800

Chen, J. L., Wilson, C. R., Blankenship, D., and Tapley, B. D.: Accelerated Antarctic ice loss from satellite gravity measurements, *Nat.Geosci.*, 2, 859–862, <https://doi.org/10.1038/ngeo694>, 2009.

805 Chen, X., Virkkula, A., Kerminen, V.-M., Manninen, H. E., Busetto, M., Lanconelli, C., Lupi, A., Vitale, V., Del Guasta, M., Grigioni, P., Väänänen, R., Duplissy, E.-M., Petäjä, T., and Kulmala, M.: Features in air ions measured by an air ion spectrometer (AIS) at Dome C, *Atmos. Chem. Phys.*, 17, 13783–13800, <https://doi.org/10.5194/acp-17-13783-2017>, 2017.

810 Chown, S.L. & Convey, P. (2007) Spatial and temporal variability across life's hierarchies in the terrestrial Antarctic. *Philosophical Transactions of the Royal Society B: Biological Sciences*, 362: 2307–2331

Cunliffe, M.; Engel, A.; Frka, S.; Gasparovic, B.; Guitart, C.; Murrell, J.C.; Salter, M.; Stolle, C. Sea surface microlayers: A unified physicochemical and biological perspective of the air-ocean interface. *Prog. Oceanogr.* 2013, 1109, 104–116.

815 Dall'Osto, M., Ovadnevaite, J., Paglione, M., Beddows, D. C. S., Ceburnis, D., Cree, C., Cortés, P., Zamanillo, M., Nunes, S. O., Pérez, G. L., Ortega-Retuerta, E., Emelianov, M., Vaqué, D., Marrasé, C., Estrada, M., Sala, M. M., Vidal, M., Fitzsimons, M. F., Beale, R., Airs, R., Rinaldi, M., Decesari, S., Facchini, M. C., Harrison, R. M., O'Dowd, C. and Simó, R.: Antarctic sea ice region as a source of biogenic organic nitrogen in aerosols, *Sci. Rep.*, 7(1), 1–10, doi:10.1038/s41598-017-06188-x, 2017a.

820 Dall'Osto, M., Beddows, D. C. S., Tunved, P., Krejci, R., Ström, J., Hansson, H. C., Yoon, Y. J., Park, K. T., Becagli, S., Udisti, R., Onasch, T., O'Dowd, C. D., Simó, R. and Harrison, R. M.: Arctic sea ice melt leads to atmospheric new particle formation, *Sci. Rep.*, 7(1), 1–10, doi:10.1038/s41598-017-03328-1, 2017b.

830 Dall'Osto, M., Geels, C., Beddows, D. C. S., Boertmann, D., Lange, R., Nøjgaard, J. K., Harrison, R. M., Simo, R., Skov, H. and Massling, & A.: Regions of open water and melting sea ice drive new particle formation in North East Greenland OPEN, *Sci. Rep.*, 8, 6109, doi:10.1038/s41598-018-24426-8, 2018.

835 Dall'Osto, M., Airs, R. L., Beale, R., Cree, C., Fitzsimons, M. F., Beddows, D., Harrison, R. M., Ceburnis, D., O'Dowd, C., Rinaldi, M., Paglione, M., Nenes, A., Decesari, S. and Simó, R.: Simultaneous Detection of Alkylamines in the Surface Ocean and Atmosphere of the Antarctic Sympagic Environment, *ACS Earth Sp. Chem.*, 3(5), 854–862, doi:10.1021/acsearthspacechem.9b00028, 2019a.

840 Dall'Osto, M., Beddows, D. C. S., Tunved, P., Harrison, R. M., Lupi, A., Vitale, V., Becagli, S., Traversi, R., Park, K. T., Jun Yoon, Y., Massling, A., Skov, H., Lange, R., Strom, J. and Krejci, R.: Simultaneous measurements of aerosol size distributions at three sites in the European high Arctic, *Atmos. Chem. Phys.*, 19(11), 7377–7395, doi:10.5194/acp-19-7377-2019, 2019b.

845 Dall'Osto, Manuel, Ana Sotomayor-Garcia, Miguel Cabrera-Brufau, Elisa Berdalet, Dolores Vaqué, Sebastian Zeppenfeld, Manuela van Pinxteren, Hartmut Herrmann, Heike Wex,



- 850 Matteo Rinaldi, Marco Paglione, David Beddows, Roy Harrison, Conxita Avila, Rafael P. Martin-Martin, Jiyeon Park, Andrés Barbosa, Leaching material from Antarctic seaweeds and penguin guano affects cloud-relevant aerosol production, *Science of The Total Environment*, Volume 831, 2022, 154772, ISSN 0048-9697, <https://doi.org/10.1016/j.scitotenv.2022.154772>.
- 855 Decesari, S., Paglione, M., Rinaldi, M., Dall'Osto, M., Simó, R., Zanca, N., Volpi, F., Facchini, M. C., Hoffmann, T., Götz, S., Kampf, C. J., O'Dowd, C., Ceburnis, D., Ovadnevaite, J., and Tagliavini, E.: Shipborne measurements of Antarctic submicron organic aerosols: an NMR perspective linking multiple sources and bioregions, *Atmos. Chem. Phys.*, 2020, 20, 4193–4207, <https://doi.org/10.5194/acp-20-4193-2020>
- 860 De Leeuw, G., Andreas, E. L., Anguelova, M. D., Fairall, C. W., Lewis, E. R., O'Dowd, C., Schulz, M. and Schwartz, S. E.: Production flux of sea spray aerosol, *Rev. Geophys.*, 49(2), 1–39, doi:10.1029/2010RG000349, 2011.
- 865 Draxler, R. R. and Rolph, G. D.: HYSPLIT (HYbrid Single-Particle Lagrangian Integrated Trajectory) Model access via NOAA ARL READY Website, [online] Available from: <https://ready.arl.noaa.gov/HYSPLIT.php>, 2010.
- Fetterer, F., Knowles, K., Meier, W. N., Savoie, M., and Wind-nagel, A. K.: Sea Ice Index, Version 3. [Indicate subset used]. Boulder, Colorado USA, NSIDC: National Snow and Ice Data Center, <https://doi.org/https://doi.org/10.7265/N5K072F8>.2019, 2017, updated daily.
- 870 Fiebig, M., Hirdman, D., Lunder, C. R., Ogren, J. A., Solberg, S., Stohl, A., and Thompson, R. L.: Annual cycle of Antarctic baseline aerosol: controlled by photooxidation-limited aerosol formation, *Atmos. Chem. Phys.*, 14, 3083–3093, <https://doi.org/10.5194/acp-14-3083-2014>, 2014.
- 875 Fossum, K. N., Ovadnevaite, J., Ceburnis, D., Dall'Osto, M., Marullo, S., Bellacicco, M., Simó, R., Liu, D., Flynn, M., Zuend, A. and O'Dowd, C.: Summertime Primary and Secondary Contributions to Southern Ocean Cloud Condensation Nuclei, *Sci. Rep.*, 8(1), 1–14, doi:10.1038/s41598-018-32047-4, 2018.
- 880 Frey, M. M., Norris, S. J., Brooks, I. M., Anderson, P. S., Nishimura, K., Yang, X., Jones, A. E., Nerentorp Mastromonaco, M. G., Jones, D. H. and Wolff, E. W.: First direct observation of sea salt aerosol production from blowing snow above sea ice, *Atmos. Chem. Phys.*, 20(4), 2549–2578, doi:10.5194/acp-20-2549-2020, 2020.
- 885 Gantt, B. and Meskhidze, N.: The physical and chemical characteristics of marine primary organic aerosol: A review, *Atmos. Chem. Phys.*, 13(8), 3979–3996, doi:10.5194/acp-13-3979-2013, 2013.



- 890 Giordano, M. R., Kalnajs, L. E., Douglas Goetz, J., Avery, A. M., Katz, E., May, N. W.,
Leemon, A., Mattson, C., Pratt, K. A. and DeCarlo, P. F.: The importance of blowing snow to
halogen-containing aerosol in coastal Antarctica: Influence of source region versus wind
speed, *Atmos. Chem. Phys.*, 18(22), 16689–16711, doi:10.5194/acp-18-16689-2018, 2018.
- 895 Gras, L. J. and Keywood, M.: Cloud condensation nuclei over the Southern Ocean: Wind
dependence and seasonal cycles, *Atmos. Chem. Phys.*, 17(7), 4419–4432, doi:10.5194/acp-
17-4419-2017, 2017.
- 900 Gong, X., Zhang, J., Croft, B., Yang, X., Frey, M.M., Bergner, N., Chang, R.Y.-W.,
Creamean, J.M., Kuang, C., Martin, R.V., Ranjithkumar, A., Sedlacek, A.J., Uin, J., Willmes,
S., Zawadowicz, M.A., Pierce, J.R., Shupe, M.D., Schmale, J., Wang, J., 2023. Arctic
warming by abundant fine sea salt aerosols from blowing snow. *Nat. Geosci.* 16, 768–774.
<https://doi.org/10.1038/s41561-023-01254-8>
- 905 Hamilton, D. S., Lee, L. A., Pringle, K. J., Reddington, C. L., Spracklen, D. V. and Carslaw,
K. S.: Occurrence of pristine aerosol environments on a polluted planet, *Proc. Natl. Acad.
Sci. U. S. A.*, 111(52), 18466–18471, doi:10.1073/pnas.1415440111, 2014.
- 910 Hara, K., Osada, K., Nishita-Hara, C., and Yamanouchi, T.: Sea-
sonal variations and vertical features of aerosol particles in the Antarctic troposphere, *Atmos. Chem. Phys.*, 11,
5471–5484, <https://doi.org/10.5194/acp-11-5471-2011>, 2011
- 915 Hara, K., Nishita-Hara, C., Osada, K., Yabuki, M., and Yamanouchi, T.: Characterization of
aerosol number size distributions and their effect on cloud properties at Syowa Station,
Antarctica, *Atmos. Chem. Phys.*, 21, 12155–12172, [https://doi.org/10.5194/acp-21-12155-
2021](https://doi.org/10.5194/acp-21-12155-2021), 2021.
- 920 Heinrichs, M.E. et al. (2024). Breaking the Ice: A Review of Phages in Polar Ecosystems. In:
Tumban, E. (eds) *Bacteriophages. Methods in Molecular Biology*, vol 2738. Humana, New
York, NY. https://doi.org/10.1007/978-1-0716-3549-0_3
- 925 Humphries, R. S., Schofield, R., Keywood, M. D., Ward, J., Pierce, J. R., Gionfriddo, C. M.,
Tate, M. T., Krabbenhoft, D. P., Galbally, I. E., Molloy, S. B., Klekociuk, A. R., John-
ston, P. V., Kreher, K., Thomas, A. J., Robinson, A. D., Har-
ris, N. R. P., Johnson, R., and Wilson,
S. R.: Boundary layer new particle formation over East Antarctic sea ice – possible Hg-
driven nucleation?, *Atmos. Chem. Phys.*, 15, 13339–13364, [https://doi.org/10.5194/acp-15-
13339-2015](https://doi.org/10.5194/acp-15-13339-2015), 2015
- 930 Humphries, R. S., Keywood, M. D., Ward, J. P., Harnwell, J., Alexander, S. P., Klekociuk, A.
R., Hara, K., McRobert, I. M., Protat, A., Alroe, J., Cravigan, L. T., Miljevic, B., Ristovski, Z.
D., Schofield, R., Wilson, S. R., Flynn, C. J., Kulkarni, G. R., Mace, G. G., McFarquhar, G.
M., Chambers, S. D., Williams, A. G., and Griffiths, A. D.: Measurement report:
Understanding the seasonal cycle of Southern Ocean aerosols, *Atmos. Chem. Phys.*, 23,
3749–3777, <https://doi.org/10.5194/acp-23-3749-2023>, 2023.



- 935 He, X.-C., Simon, M., Iyer, S., Xie, H.-B., Rörup, B., Shen, J., Finkenzeller, H., Stolzenburg, D., Zhang, R., Baccarini, A., Tham, Y. J., Wang, M., Amanatidis, S., Piedehierro, A. A., Amorim, A., Baalbaki, R., Brasseur, Z., Caudillo, L., Chu, B., Dada, L., Duplissy, J., El Haddad, I., Flagan, R. C., Granzin, M., Hansel, A., Heinritzi, M., Hofbauer, V., Jokinen, T., Kempainen, D., Kong, W., Krechmer, J., Kürten, A., Lamkaddam, H., Lopez, B., Ma, F.,
- 940 Mahfouz, N. G. A., Makhmutov, V., Manninen, H. E., Marie, G., Marten, R., Massabò, D., Mauldin, R. L., Mentler, B., Onnela, A., Petäjä, T., Pfeifer, J., Philippov, M., Ranjithkumar, A., Rissanen, M. P., Schobesberger, S., Scholz, W., Schulze, B., Surdu, M., Thakur, R. C., Tomé, A., Wagner, A. C., Wang, D., Wang, Y., Weber, S. K., Welti, A., Winkler, P. M., Zauner-Wieczorek, M., Baltensperger, U., Curtius, J., Kurtén, T., Worsnop, D. R., Volkamer, R., Lehtipalo, K., Kirkby, J., Donahue, N. M., Sipilä, M., and Kulmala, M.: Iodine oxoacids enhance nucleation of sulfuric acid particles in the atmosphere, *Science*, 382, 1308-1314, [10.1126/science.adh2526](https://doi.org/10.1126/science.adh2526), 2023.
- 950 Heintzenberg, J, Covert, DS and Van Dingenen, R. 2000. Size distribution and chemical composition of marine aerosols: A compilation and review. *Tellus*, 52B: 1104–1122. DOI: <https://doi.org/10.1034/j.1600-0889.2000.00136.x>
- 955 Heintzenberg, J, Legrand, M, Gao, Y, Hara, K, Huang, S, Humphries, RS, Kamra, AK, Keywood, MD and Sakerin, SM. 2023. Spatio-Temporal Distributions of the Natural Non-Sea-Salt Aerosol Over the Southern Ocean and Coastal Antarctica and Its Potential Source Regions. *Tellus B: Chemical and Physical Meteorology*, 75(1): 47–64. DOI: <https://doi.org/10.16993/tellusb.1869>
- 960 Herenz, P., Wex, H., Mangold, A., Laffineur, Q., Gorodetskaya, I. V., Fleming, Z. L., Panagi, M., and Stratmann, F.: CCN measurements at the Princess Elisabeth Antarctica research station during three austral summers, *Atmos. Chem. Phys.*, 19, 275–294, <https://doi.org/10.5194/acp-19-275-2019>, 2019.
- 965 Hoffmann, E. H., Tilgner, A., Schrödner, R., Bräuer, P., Wolke, R. and Herrmann, H.: An advanced modeling study on the impacts and atmospheric implications of multiphase dimethyl sulfide chemistry, *Proc. Natl. Acad. Sci. U. S. A.*, 113(42), 11776–11781, doi:10.1073/pnas.1606320113, 2016.
- 970 Hoppel, W. A., Frick, G. M., and Fitzgerald, J. W.: Marine boundary layer measurements of new-particle formation and the effects of non-precipitating clouds have on aerosol size distribution, *J. Geophys. Res.*, 99, 14443–14459, 1994
- 975 Humphries, R. S., Keywood, M. D., Gribben, S., McRobert, I. M., Ward, J. P., Selleck, P., Taylor, S., Harnwell, J., Flynn, C., Kulkarni, G. R., Mace, G. G., Protat, A., Alexander, S. P., and McFarquhar, G.: Southern Ocean latitudinal gradients of cloud condensation nuclei, *Atmos. Chem. Phys.*, 21, 12757–12782, <https://doi.org/10.5194/acp-21-12757-2021>, 2021
- 980 Humphries, R. S., Keywood, M. D., Ward, J. P., Harnwell, J., Alexander, S. P., Klekociuk, A. R., Hara, K., McRobert, I. M., Protat, A., Alroe, J., Cravigan, L. T., Miljevic, B., Ristovski, Z. D., Schofield, R., Wilson, S. R., Flynn, C. J., Kulkarni, G. R., Mace, G. G., McFarquhar, G. M., Chambers, S. D., Williams, A. G., and Griffiths, A. D.: Measurement report:



Understanding the seasonal cycle of Southern Ocean aerosols, *Atmos. Chem. Phys.*, 23, 3749–3777, <https://doi.org/10.5194/acp-23-3749-2023>, 2023.

- 985 Hsu, Y., Holsen, T. M. and Hopke, P. K.: Comparison of hybrid receptor models to locate PCB sources in Chicago, *Atmos. Environ.*, 37, 545–562, 2003.
- Ice, C. U. N.: IMS Daily Northern Hemisphere Snow and Ice Analysis at 1 km, 4 km, and 24 km Resolutions, Version 1. Boulder, Colorado USA. NSIDC: National Snow and Ice Data Center, US Natl. Ice Cent., doi:<https://doi.org/10.7265/N52R3PMC>, 2008.
- Ito, T.: Size distribution of Antarctic submicron aerosols, *Tellus B*, 45, 145–59, 1993.
- 990 James, I. M.: The Antarctic drainage flow: implications for hemi- spheric flow on the Southern Hemisphere, *Antarct. Sci.*, 1, 279– 290, 1989.
- Jang, E., Park, K. T., Jun Yoon, Y., Kim, T. W., Hong, S. B., Becagli, S., Traversi, R., Kim, J. and Gim, Y.: New particle formation events observed at the King Sejong Station, Antarctic Peninsula - Part 2: Link with the oceanic biological activities, *Atmos. Chem. Phys.*, 19(11), 7595–7608, doi:10.5194/acp-19-7595-2019, 2019.
- 995 Järvinen, E., Virkkula, A., Nieminen, T., Aalto, P. P., Asmi, E., Lanconelli, C., Busetto, M., Lupi, A., Schioppo, R., Vitale, V., Mazzola, M., Petäjä, T., Kerminen, V.-M. and Kulmala, M.: Sciences ess Atmospheric Chemistry and Physics Climate of the Past Geoscientific Instrumentation Methods and Data Systems Seasonal cycle and modal structure of particle number size distribution at Dome C, Antarctica, *Atmos. Chem. Phys.*, 13, 7473–7487, doi:10.5194/acp-13-7473-2013, 2013a.
- 1000 Järvinen, E., Virkkula, A., Nieminen, T., Aalto, P. P., Asmi, E., Lanconelli, C., Busetto, M., Lupi, A., Schioppo, R., Vitale, V., Mazzola, M., Petäjä, T., Kerminen, V. M. and Kulmala, M.: Seasonal cycle and modal structure of particle number size distribution at Dome C, Antarctica, *Atmos. Chem. Phys.*, 13(15), 7473–7487, doi:10.5194/acp-13-7473-2013, 2013b.
- 1005 Jokinen, T., Sipilä, M., Kontkanen, J., Vakkari, V., Tisler, P., Duplissy, E.-M., Junninen, H., Kangasluoma, J., Manninen, H. E., Petäjä, T., Kulmala, M., Worsnop, D. R., Kirkby, J., Virkkula, A. and Kerminen, V.-M.: Ion-induced sulfuric acid–ammonia nucleation drives particle formation in coastal Antarctica, *Sci. Adv.*, 4(11), eaat9744, doi:10.1126/sciadv.aat9744, 2018.
- 1010 Kerminen, V. M., Chen, X., Vakkari, V., Petäjä, T., Kulmala, M. and Bianchi, F.: Atmospheric new particle formation and growth: Review of field observations, *Environ. Res. Lett.*, 13(10), doi:10.1088/1748-9326/aadf3c, 2018.
- 1015 Kim, J., Yoon, Y. J., Gim, Y., Kang, H. J., Choi, J. H., Park, K. and Lee, B. Y.: Seasonal variations in physical characteristics of aerosol particles at the King Sejong Station, Antarctic Peninsula, *Atmos. Chem. Phys.*, 17, 12985–12999, 2017.
- 1020 Kim, J., Jun Yoon, Y., Gim, Y., Hee Choi, J., Jin Kang, H., Park, K. T., Park, J. and Yong Lee, B.: New particle formation events observed at King Sejong Station, Antarctic Peninsula



- 1025 - Part 1: Physical characteristics and contribution to cloud condensation nuclei, *Atmos. Chem. Phys.*, 19(11), 7583–7594, doi:10.5194/acp-19-7583-2019, 2019.
- 1030 Kirkby, J., Curtius, J., Almeida, J., Dunne, E., Duplissy, J., Ehrhart, S., Franchin, A., Gagné, S., Ickes, L., Kürten, A., Kupc, A., Metzger, A., Riccobono, F., Rondo, L., Schobesberger, S., Tsagkogeorgas, G., Wimmer, D., Amorim, A., Bianchi, F., Breitenlechner, M., David, A., Dommen, J., Downard, A., Ehn, M., Flagan, R. C., Haider, S., Hansel, A., Hauser, D., Jud, W., Junninen, H., Kreissl, F., Kvashin, A., Laaksonen, A., Lehtipalo, K., Lima, J., Lovejoy, E. R., Makhmutov, V., Mathot, S., Mikkilä, J., Minginette, P., Mogo, S., Nieminen, T., Onnela, A., Pereira, P., Petäjä, T., Schnitzhofer, R., Seinfeld, J. H., Sipilä, M., Stozhkov, Y., Stratmann, F., Tomé, A., Vanhanen, J., Viisanen, Y., Vrtala, A., Wagner, P. E., Walther, H., Weingartner, E., Wex, H., Winkler, P. M., Carslaw, K. S., Worsnop, D. R., Baltensperger, U. and Kulmala, M.: Role of sulphuric acid, ammonia and galactic cosmic rays in atmospheric aerosol nucleation, *Nature*, 476(7361), 429–435, doi:10.1038/nature10343, 2011.
- 1035
- 1040 Koponen, I. K., Virkkula, A., Hillamo, R., Kerminen, V.-M., and Kulmala, M.: Number size distributions of marine aerosols: observations during a cruise between the English Channel and coast of Antarctica, *J. Geophys. Res.*, 107, 4753, <https://doi.org/10.1029/2002JD002533>, 2002.
- 1045 Korhonen, H., Carslaw, K. S., Spracklen, D. V., Mann, G. W. and Woodhouse, M. T.: Influence of oceanic dimethyl sulfide emissions on cloud condensation nuclei concentrations and seasonality over the remote Southern Hemisphere oceans: A global model study, *J. Geophys. Res. Atmos.*, 113(15), 1–16, doi:10.1029/2007JD009718, 2008.
- 1050 Lachlan-Cope, T., Beddows, D., Brough, N., Jones, A., Harrison, R., Lupi, A., Yoon, Y. J., Virkkula, A. and Dall'Osto, M.: On the annual variability of Antarctic aerosol size distributions at Halley research station, *Atmos. Chem. Phys.*, 20(7), 4461–4476, doi:10.5194/acp-2019-847, 2020.
- 1055 Lana, A., et al. (2011), An updated climatology of surface dimethylsulfide concentrations and emission fluxes in the global ocean, *Global Biogeochem. Cycles*, 25, GB1004, doi:10.1029/2010GB003850.
- 1060 Lee, S. H., Gordon, H., Yu, H., Lehtipalo, K., Haley, R., Li, Y., and Zhang, R.: New Particle Formation in the Atmosphere: From Molecular Clusters to Global Climate, *Journal of Geophysical Research: Atmospheres*, 124, 7098-7146, 10.1029/2018jd029356, 2019.
- 1065 Lapere, R., Thomas, J. L., Marelle, L., Ekman, A. M. L., Frey, M. M., Lund, M. T., et al. (2023). The representation of sea salt aerosols and their role in polar climate within CMIP6. *Journal of Geophysical Research: Atmospheres*, 128, e2022JD038235.
- 1070 Legrand, M., Yang, X., Preunkert, S. and Theys, N.: Year-round records of sea salt, gaseous, and particulate inorganic bromine in the atmospheric boundary layer at coastal (Dumont d'Urville) and central (Concordia) East Antarctic sites, *J. Geophys. Res. Atmos.*, (121), 997–1023, 2016.



- Lupu, A. and Maenhaut, W.: Application and comparison of two statistical trajectory techniques for identification of source regions of atmospheric aerosol species, *Atmospheric Environ.*, 36, 5607–5618, 2002.
- 1075
- McCoy, D. T., Burrows, S. M., Wood, R., Grosvenor, D. P., Elliott, S. M., Ma, P. L., Rasch, P. J., & Hartmann, D. L.: Natural aerosols explain seasonal and spatial patterns of Southern Ocean cloud albedo. *Science Advances*, 1(6), e1500157. <https://doi.org/10.1126/sciadv.1500157>, 2015.
- 1080
- Meskhize, N. and Nenes, A.: Phytoplankton and cloudiness in the Southern Ocean, *Science*, 314, 1419–1423, <https://doi.org/10.1126/science.1131779>, 2006
- 1085
- Mungall, E. L., Abbatt, J. P. D., Wentzell, J. J. B., Lee, A. K. Y., Thomas, J. L., Blais, M., Gosselin, M., Miller, L. A., Papakyriakou, T., Willis, M. D., and Liggio, J.: Microlayer source of oxygenated volatile organic compounds in the summertime marine Arctic boundary layer, *P. Natl. Acad. Sci. USA*, 114, 6203–6208, <https://doi.org/10.1073/pnas.1620571114>, 2017.
- 1090
- O’Dowd, C. D., Lowe, J. A., Smith, M. H., Davison, B., Hewitt, C. N. and Harrison, R. M.: Biogenic sulphur emissions and inferred non-sea-salt-sulphate particularly during Events of new particle formation in and around Antarctica, *Atlantic*, 102(DII), 1997a.
- 1095
- O’Dowd, C. D., Smith, M. H., Consterdine, I. E. and Lowe, J. A.: Marine aerosol, sea-salt, and the marine sulphur cycle: A short review, *Atmos. Environ.*, 31(1), 73–80, doi:10.1016/S1352-2310(96)00106-9, 1997b.
- 1100
- Otero, X. L., De La Peña-Lastra, S., Pérez-Alberti, A., Ferreira, T. O. and Huerta-Diaz, M. A.: Seabird colonies as important global drivers in the nitrogen and phosphorus cycles, *Nat. Commun.*, 9(1), doi:10.1038/s41467-017-02446-8, 2018.
- 1105
- Paglione, M., Beddows, D. C. S., Jones, A., Lachlan-Cope, T., Rinaldi, M., Decesari, S., Manarini, F., Russo, M., Mansour, K., Harrison, R. M., Mazzanti, A., Tagliavini, E., and Dall’Osto, M.: Simultaneous organic aerosol source apportionment at two Antarctic sites reveals large-scale and eco-region specific components, *EGUsphere [preprint]*, <https://doi.org/10.5194/egusphere-2023-2275>, 2023.
- 1110
- Park, J., Kang, H., Gim, Y., Jang, E., Park, K.-T., Park, S., Jung, C. H., Ceburnis, D., O’Dowd, C., and Yoon, Y. J.: New particle formation leads to enhanced cloud condensation nuclei concentrations on the Antarctic Peninsula, *Atmos. Chem. Phys.*, 23, 13625–13646, <https://doi.org/10.5194/acp-23-13625-2023>, 2023.
- Peck, L.S., 2018. Antarctic marine biodiversity: adaptations, environments and responses to change. *Oceanogr. Mar. Biol. Annu. Rev.* 56, 105–236.



- 1115 Quinn, P. K. and Bates, T. S.: The case against climate regulation via oceanic phytoplankton sulphur emissions, *Nature*, 480, 51–56, <https://doi.org/10.1038/nature10580>, 2011.
- Rankin, A. M. and Wolff, E. W.: A year-long record of size-segregated aerosol composition at Halley, Antarctica, *J. Geophys. Res. Atmos.*, 108(24), 1–12, doi:10.1029/2003jd003993, 2003.
- 1120
- Reddington, C. L., Carslaw, K. S., Stier, P., Schutgens, N., Coe, H., Liu, D., Allan, J., Browse, J., Pringle, K. J., Lee, L. A., Yoshioka, M., Johnson, J. S., Regayre, L. A., Spracklen, D. V., Mann, G. W., Clarke, A., Hermann, M., Henning, S., Wex, H., Kristensen, T. B., Leaitch, W. R., Pöschl, U., Rose, D., Andreae, M. O., Schmale, J., Kondo, Y., Oshima, N., Schwarz, J. P., Nenes, A., Anderson, B., Roberts, G. C., Snider, J. R., Leck, C., Quinn, P. K., Chi, X., Ding, A., Jimenez, J. L. and Zhang, Q.: The global aerosol synthesis and science project (GASSP): Measurements and modeling to reduce uncertainty, *Bull. Am. Meteorol. Soc.*, 98(9), 1857–1877, doi:10.1175/BAMS-D-15-00317.1, 2017.
- 1125
- 1130
- Riddick, S. N., Dragosits, U., Blackall, T. D., Daunt, F., Wanless, S., and Sutton, M. A.: The global distribution of ammonia emissions from seabird colonies, *Atmos. Environ.*, 55, 319–327, doi:10.1016/j.atmosenv.2012.02.052, 2012.
- 1135
- Rinaldi, M., Paglione, M., Decesari, S., Harrison, R. M., Beddows, D. C., Ovadnevaite, J., Ceburnis, D., O'Dowd, C. D., Simó, R., and Dall'Osto, M.: Contribution of Water-Soluble Organic Matter from Multiple Marine Geographic Eco-Regions to Aerosols around Antarctica, *Environ. Sci. Technol.*, 54, 7807–7817, <https://doi.org/10.1021/acs.est.0c00695>, 2020
- 1140
- Ronowicz, M., Peña Cantero, A.L., Mercado Casares, B., Kuklinski, P., Soto Àngel, J.J., 2019. Assessing patterns of diversity, bathymetry and distribution at the poles using hydrozoa (Cnidaria) as a model group. *Hydrobiologia* 833, 25–51. <https://doi.org/10.1007/s10750-018-3876-5>.
- 1145
- Saliba, G., Sanchez, K. J., Russell, L. M., Twohy, C. H., Roberts, G. C., Lewis, S., Dedrick, J., McCluskey, C. S., Moore, K., DeMott, P. J., Toohey, D. W.: Organic composition of three different size ranges of aerosol particles over the Southern Ocean, *Aerosol Science and Technology*, 55:3, 268-288, DOI: 10.1080/02786826.2020.1845296, 2021.
- 1150
- Schmale, J., Schneider, J., Nemitz, E., Tang, Y. S., Dragosits, U., Blackall, T. D., Trathan, P. N., Phillips, G. J., Sutton, M., and Braban, C. F.: Sub-Antarctic marine aerosol: dominant contributions from biogenic sources, *Atmos. Chem. Phys.*, 13, 8669–8694, <https://doi.org/10.5194/acp-13-8669-2013>, 2013.
- 1155



Shaw, G. E.: Considerations on the Origin and Properties of the Antarctic Aerosol, *Rev. Geophys.*, 17, 1983–1998, 1988

- 1160 Sipilä, M., Sarnela, N., Jokinen, T., Henschel, H., Junninen, H., Kontkanen, J., Richters, S., Kangasluoma, J., Franchin, A., Peräkylä, O., Rissanen, M. P., Ehn, M., Vehkamäki, H., Kurten, T., Berndt, T., Petäjä, T., Worsnop, D., Ceburnis, D., Kerminen, V. M., Kulmala, M. and O'Dowd, C.: Molecular-scale evidence of aerosol particle formation via sequential addition of HIO₃, *Nature*, 537(7621), 532–534, doi:10.1038/nature19314, 2016.
- 1165 Terauds, A., S. L. Chown, F. Morgan, H. J. Peat, D. J. Watts, H. Keys, P. Convey, and D. M. Bergstrom. (2012) Conservation biogeography of the Antarctic. *Diversity and Distributions* 18:726-741.
- 1170 Terauds, A., and Lee, J. R. (2016) Antarctic biogeography revisited: updating the Antarctic conservation biogeographic regions. *Diversity and Distributions* 22:836-840.
- 1175 Turner, J., Colwell, S. R., Marshall, G. J., Lachlan-Cope, T. A., Carleton, A. M., Jones, P. D., Lagun, V., Reid, P. A. and Iagovkina, S.: Antarctic climate change during the last 50 years, *Int. J. Climatol.*, 25(3), 279–294, doi:10.1002/joc.1130, 2005.
- 1180 Vaqué, D.; Boras, J.A.; Arrieta, J.M.; Agustí, S.; Duarte, C.M.; Sala, M.M. Enhanced Viral Activity in the Surface Microlayer of the Arctic and Antarctic Oceans. *Microorganisms* 2021, 9, 317. <https://doi.org/10.3390/microorganisms9020317>
- 1185 Virkkula, A., Grythe, H., Backman, J., Petäjä, T., Busetto, M., Lanconelli, C., Lupi, A., Becagli, S., Traversi, R., Severi, M., Vitale, V., Sheridan, P., and Andrews, E.: Aerosol optical properties calculated from size distributions, filter samples and absorption photometer data at Dome C, Antarctica, and their relationships with seasonal cycles of sources, *Atmos. Chem. Phys.*, 22, 5033–5069, <https://doi.org/10.5194/acp-22-5033-2022>, 2022.
- 1190 Yang, X., Frey, M. M., Rhodes, R. H., Norris, S. J., Brooks, I. M., Anderson, P. S., Nishimura, K., Jones, A. E., and Wolff, E. W.: Sea salt aerosol production via sublimating wind-blown saline snow particles over sea ice: parameterizations and relevant microphysical mechanisms, *Atmos. Chem. Phys.*, 19, 8407–8424, <https://doi.org/10.5194/acp-19-8407-2019>, 2019.
- 1195 Wang, M., Xiao, M., Bertozzi, B., Marie, G., Rörup, B., Schulze, B., Bardakov, R., He, X.-C., Shen, J., Scholz, W., Marten, R., Dada, L., Baalbaki, R., Lopez, B., Lamkaddam, H., Manninen, H. E., Amorim, A., Ataei, F., Bogert, P., Brasseur, Z., Caudillo, L., De Menezes, L.-P., Duplissy, J., Ekman, A. M. L., Finkenzeller, H., Carracedo, L. G., Granzin, M., Guida, R., Heinritzi, M., Hofbauer, V., Höhler, K., Korhonen, K., Krechmer, J. E., Kürten, A., Lehtipalo, K., Mahfouz, N. G. A., Makhmutov, V., Massabò, D., Mathot, S., Mauldin, R. L., Mentler, B., Müller, T., Onnela, A., Petäjä, T., Philippov, M., Piedehierro, A. A., Pozzer, A., Ranjithkumar, A., Schervish, M., Schobesberger, S., Simon, M., Stozhkov, Y., Tomé, A., Umo, N. S., Vogel, F., Wagner, R., Wang, D. S., Weber, S. K., Welti, A., Wu, Y., Zauner-Wieczorek, M., Sipilä, M., Winkler, P. M., Hansel, A., Baltensperger, U., Kulmala, M., Flagan, R. C., Curtius, J., Riipinen, I., Gordon, H., Lelieveld, J., El-Haddad, I., Volkamer, R.,



- 1205 Worsnop, D. R., Christoudias, T., Kirkby, J., Möhler, O. and Donahue, N. M.: Synergistic HNO₃–H₂SO₄–NH₃ upper tropospheric particle formation, *Nature*, 605(7910), 483–489, doi:10.1038/s41586-022-04605-4, 2022.
- 1210 Weller, R., Minikin, A., Wagenbach, D., and Dreiling, V.: Characterization of the inter-annual, seasonal, and diurnal variations of condensation particle concentrations at Neumayer, Antarctica, *Atmos. Chem. Phys.*, 11, 13243–13257, <https://doi.org/10.5194/acp-11-13243-2011>, 2011.
- 1215 Weller, R., Schmidt, K., Teinilä, K., and Hillamo, R.: Natural new particle formation at the coastal Antarctic site Neumayer, *Atmos. Chem. Phys.*, 15, 11399–11410, <https://doi.org/10.5194/acp-15-11399-2015>, 2015.
- 1220 Weller, R., Legrand, M., and Preunkert, S.: Size distribution and ionic composition of marine summer aerosol at the continental Antarctic site Kohnen, *Atmos. Chem. Phys.*, 18, 2413–2430, <https://doi.org/10.5194/acp-18-2413-2018>, 2018.
- 1225 Wiencke and Amsler, 2012 C. Wiencke, C.D. Amsler *Seaweeds and Their Communities in Polar Regions* Springer, Berlin, Heidelberg (2012), pp. 265-291, 10.1007/978-3-642-28451-9_13
- 1230 Wohl, C., Li, Q., Cuevas, C. A., Fernandez, R. P., Yang, M., Saiz-Lopez, A., and Simó, R.: Marine biogenic emissions of benzene and toluene and their contribution to secondary organic aerosols over the polar oceans, *Science Advances*, 9, eadd9031, 10.1126/sciadv.add9031,

1235



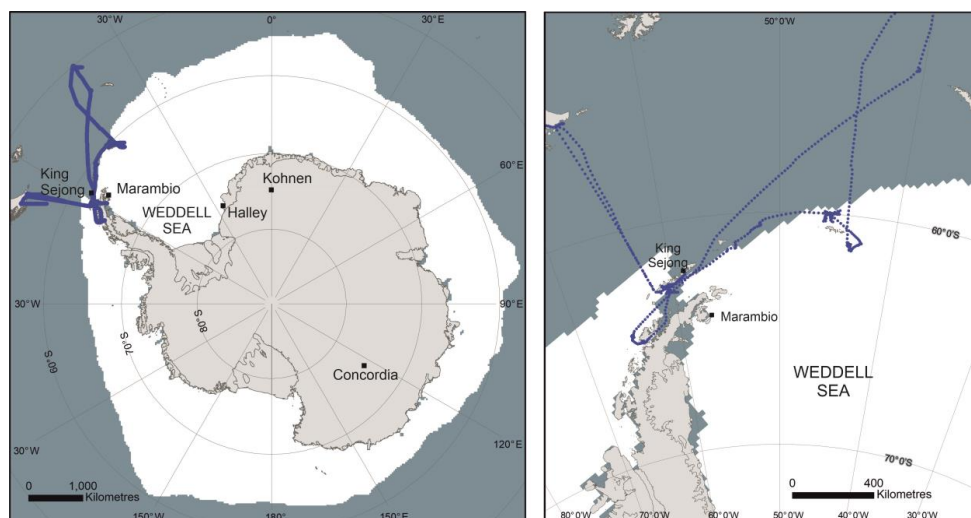
1240

Site	Lat	Lon	Elevation a.s.l. (m)
King Sejong	-62.2	-58.8	10
Marambio	-64.2	-56.6	198
Concordia/Dome C	-75.1	123.3	3233
Halley	-75.6	-26.2	30

1245 Table 1: Latitude & longitude of each site

1250

1255



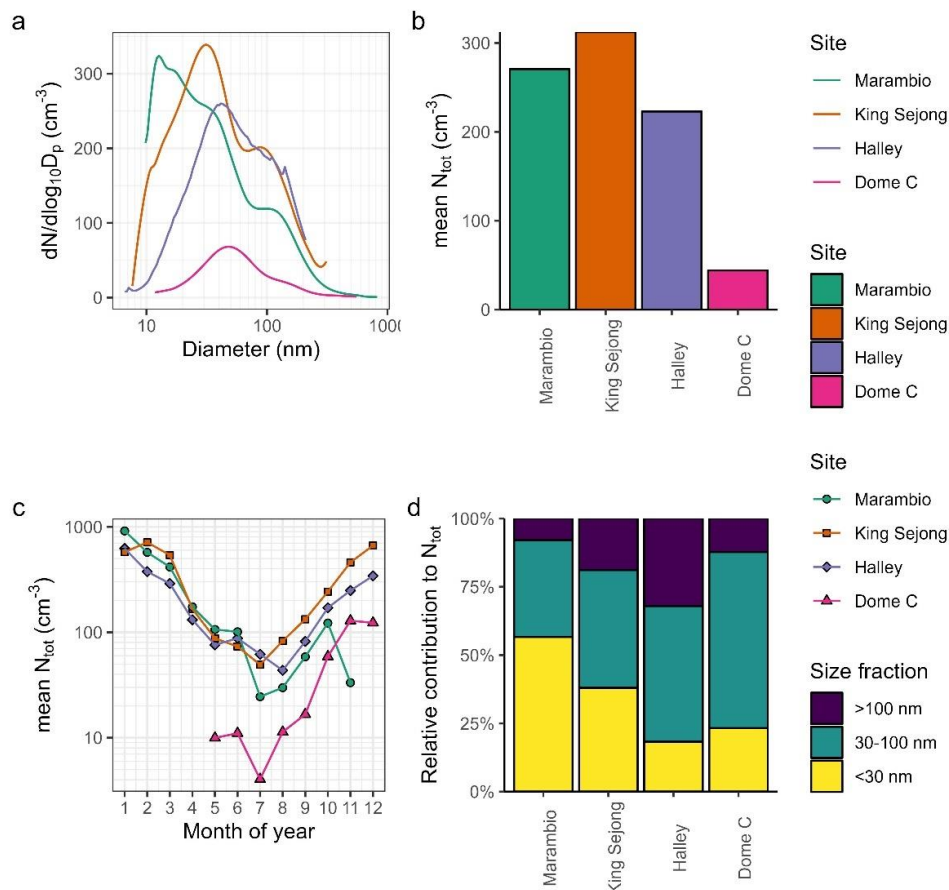
1260

Figure 1 Map of the sampling stations (Halley, Marambio, Concordia/Dome C, King Sejong) for the year dataset collected in 2015. Additional, data for shorter period are intercompared at Kohnen (Weller et al., 2018) and during the PEGASO cruise (Dall'Osto et al., 2017, blue line the PEGASO cruise track). Please note that the sea ice extent is the median September extent from 1981 to 2010 (data are from the National Snow and Ice Data Center – NSIDC – at <https://nsidc.org/data/>, last access: 17 March 2024, Fetterer et al., 2017).

1270



1275



1280

Figure 2: Features of particle PNSD data for four Antarctic sites, showing (a) mean particle PNSD per site, (b) mean particle count per site, (c) seasonal variation in particle count per site, and (d) contribution of different size fractions to particle count per site. Only data from the same time period (April-December) are intercompared and presented in Figure 2a,b,d, whereas all the temporal trend is presented in Figure 2c.

1285

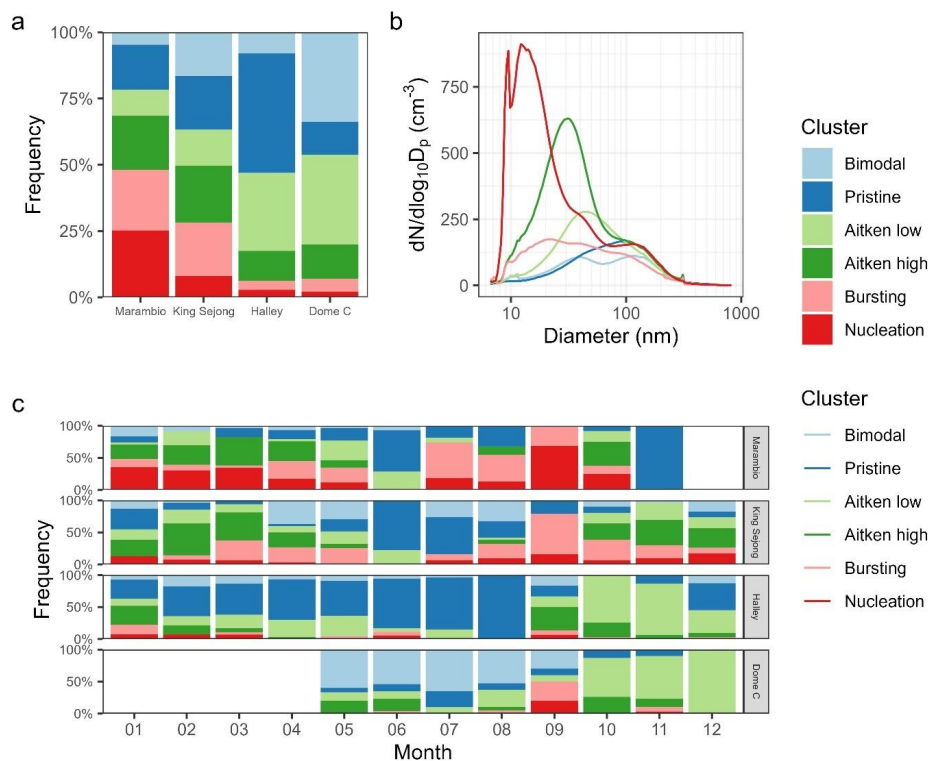


Figure 3: Cluster analysis results, showing (a) average frequency of each cluster per site, (b) mean PNSD per cluster, and (c) seasonal variations in cluster frequency per site

1290

1295

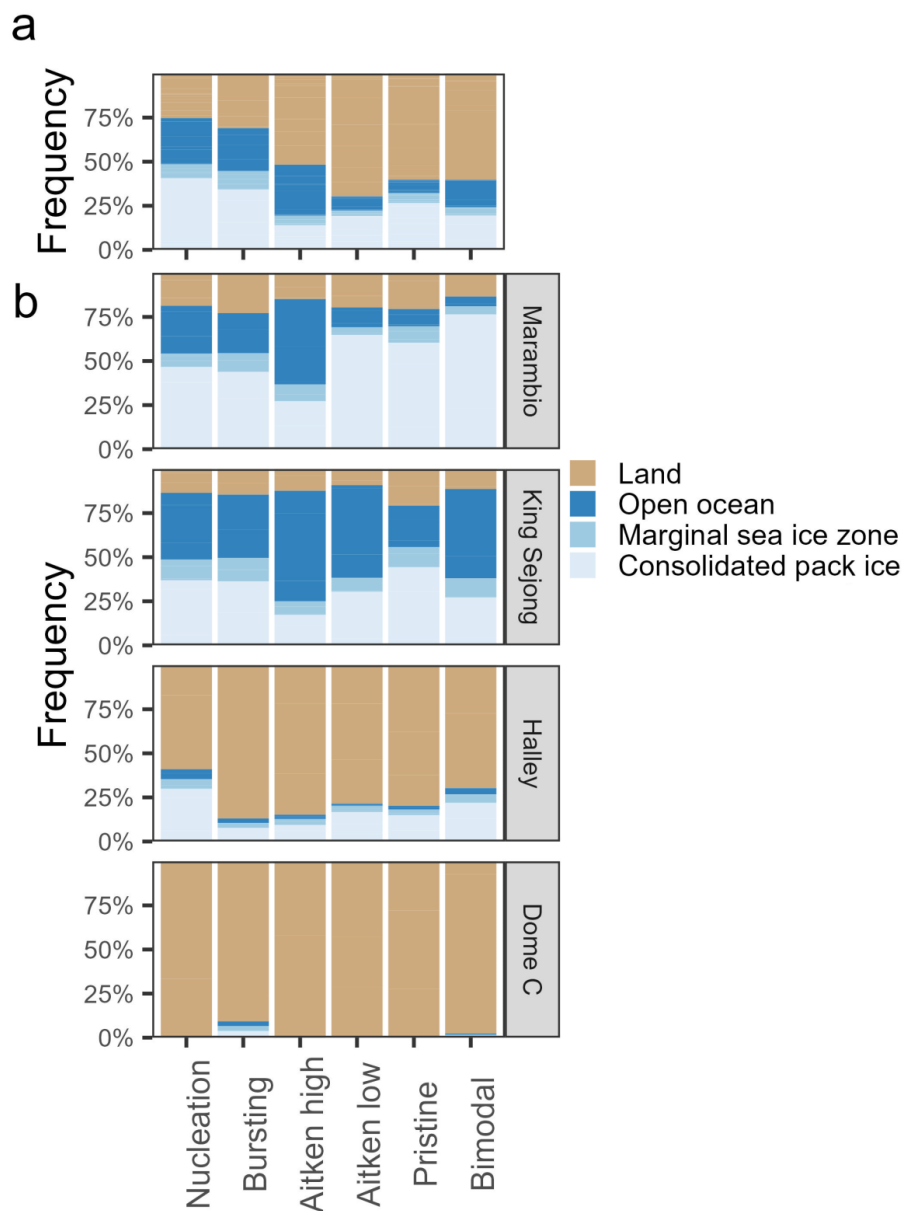
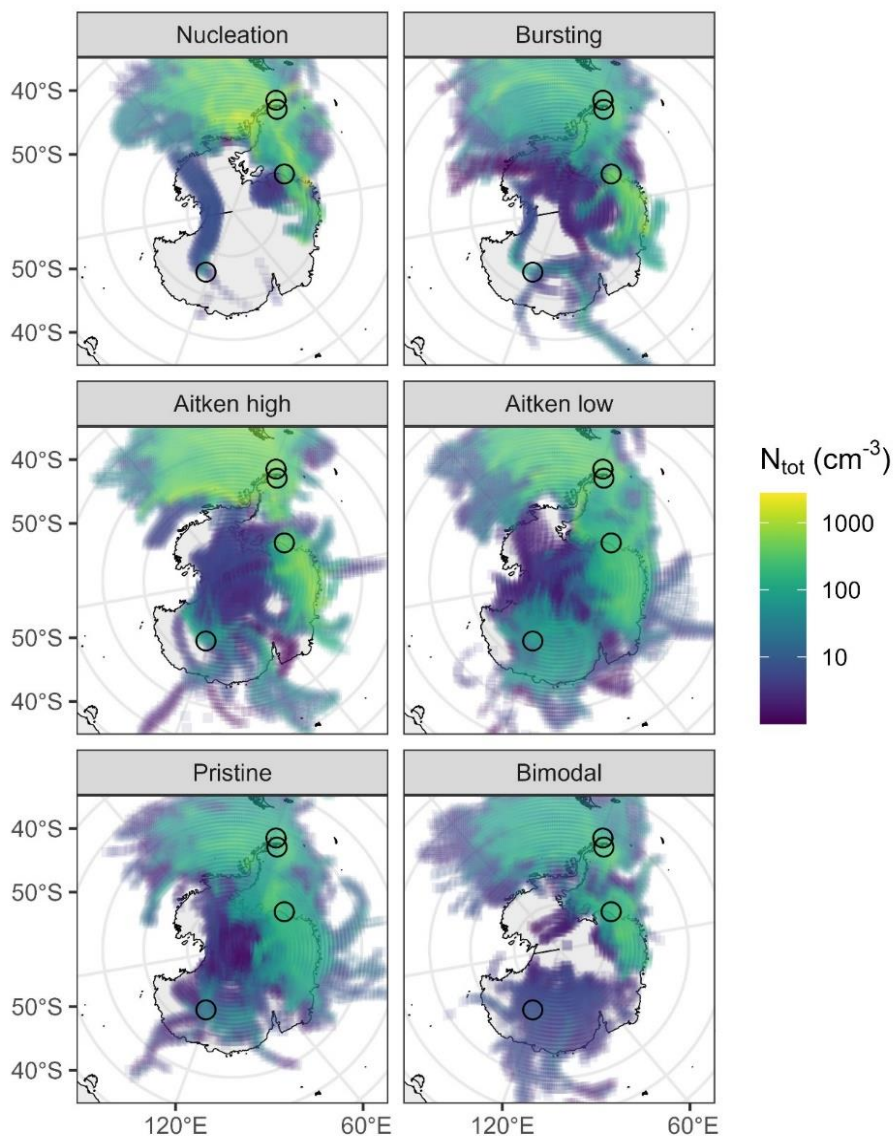
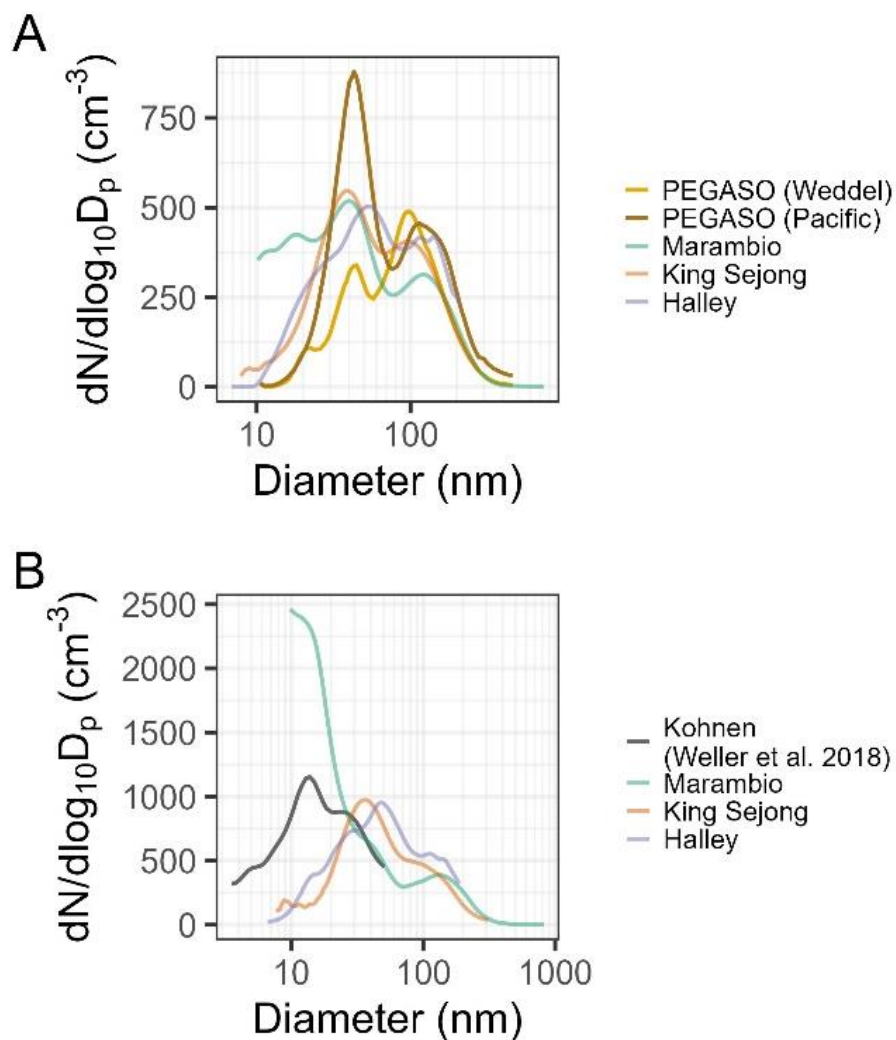


Figure 4: Land surface types associated with each cluster, showing (a) average association across all sites, and (b) association per site

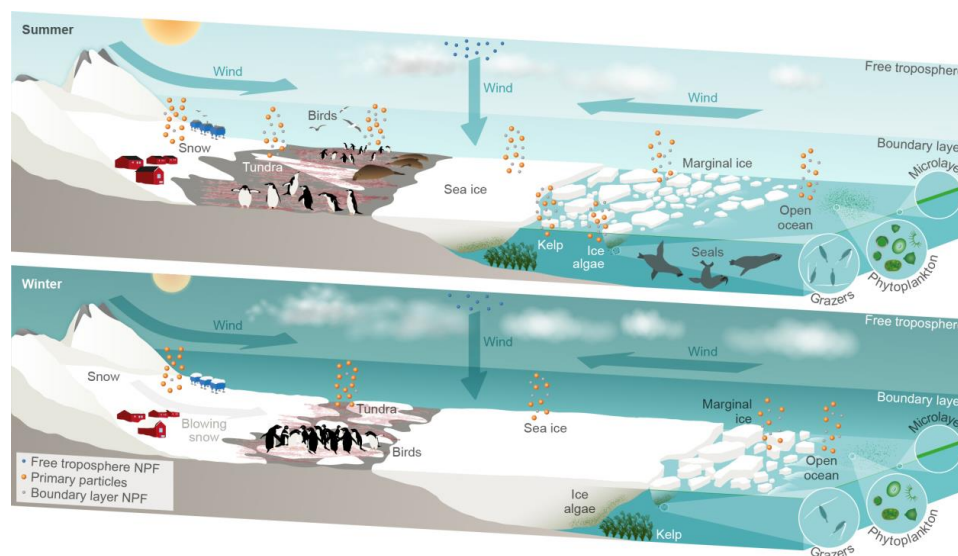


1305

Figure 5: Concentration weighted trajectory maps showing the sources of particles corresponding to each cluster. 72 hour back trajectories calculated with Hysplit



1310 Figure 6: PNSD intercomparisons: (A) PNSD from the PEGASO cruise both when
influenced from air masses from the Weddel Sea and Pacific Ocean and the stations
used for this study where overlapping data are available (Marambio, Halley and King
Sejong stations), and (B) PNSD from the Kohnen station (Weller et al., 2018) and the
stations used for this study where overlapping data are available (Marambio, Halley
1315 and King Sejong stations)



1320

Figure 7 Schematic illustrations of the sea ice, microbiota, sea-to-air emissions, and primary and secondary aerosols in Antarctica during summer (top) and winter (bottom).